# Measurement of jet pT correlations in Pb + Pb and pp collisions at sNN=2.76TeV with the ATLAS detector

ATLAS Collaboration; Newman, Paul

*DOI:*
10.1016/j.physletb.2017.09.078



*Document Version*
Publisher's PDF, also known as Version of record

*Citation for published version (Harvard):*
ATLAS Collaboration 2017, 'Measurement of jet pT correlations in Pb + Pb and pp collisions at sNN=2.76TeV with the ATLAS detector', Physical Review Letters, vol. 774, pp. 379-402.
https://doi.org/10.1016/j.physletb.2017.09.078



https://doi.org/10.1016/j.physletb.2017.09.078

Physics Letters B 774 (2017) 379–402

Contents lists available at ScienceDirect

Physics Letters B

www.elsevier.com/locate/physletb

# Measurement of jet $p_{\mathrm{T}}$ correlations in Pb+Pb and $pp$ collisions at $\sqrt{s_{\mathrm{NN}}} = 2.76$ TeV with the ATLAS detector

The ATLAS Collaboration *

ARTICLE INFO

*Article history:*
Received 29 June 2017
Received in revised form 13 September 2017
Accepted 26 September 2017
Available online 29 September 2017
Editor: D.F. Geesaman

ABSTRACT

Measurements of dijet $p_{\mathrm{T}}$ correlations in Pb+Pb and $pp$ collisions at a nucleon–nucleon centre-of-mass energy of $\sqrt{s_{\mathrm{NN}}} = 2.76$ TeV are presented. The measurements are performed with the ATLAS detector at the Large Hadron Collider using Pb+Pb and $pp$ data samples corresponding to integrated luminosities of 0.14 nb$^{-1}$ and 4.0 pb$^{-1}$, respectively. Jets are reconstructed using the anti-$k_t$ algorithm with radius parameter values $R = 0.3$ and $R = 0.4$. A background subtraction procedure is applied to correct the jets for the large underlying event present in Pb+Pb collisions. The leading and subleading jet transverse momenta are denoted $p_{\mathrm{T}_1}$ and $p_{\mathrm{T}_2}$. An unfolding procedure is applied to the two-dimensional $(p_{\mathrm{T}_1}, p_{\mathrm{T}_2})$ distributions to account for experimental effects in the measurement of both jets. Distributions of $(1/N)\mathrm{d}N/\mathrm{d}x_{\mathrm{J}}$, where $x_{\mathrm{J}} = p_{\mathrm{T}_2}/p_{\mathrm{T}_1}$, are presented as a function of $p_{\mathrm{T}_1}$ and collision centrality. The distributions are found to be similar in peripheral Pb+Pb collisions and $pp$ collisions, but highly modified in central Pb+Pb collisions. Similar features are present in both the $R = 0.3$ and $R = 0.4$ results, indicating that the effects of the underlying event are properly accounted for in the measurement. The results are qualitatively consistent with expectations from partonic energy loss models.



## 1. Introduction

Jets have long been considered an important tool for studying the matter produced in ultra-relativistic heavy-ion collisions. In these collisions, a hot medium of deconfined colour charges is produced, known as the quark–gluon plasma (QGP). Jets produced in the initial stage of the collision lose energy as they propagate through the medium. This phenomenon, known as *jet quenching*, was first observed at the Relativistic Heavy Ion Collider (RHIC) [1,2]. Early measurements using fully reconstructed jets in Pb+Pb collisions at the LHC provided a direct observation of this phenomenon [3]. In Pb+Pb collisions the transverse momentum ($p_{\mathrm{T}}$) balance between two jets was found to be distorted, resulting from configurations in which the two jets suffer different amounts of energy loss. This measurement was the experimental confirmation of some of the initial pictures of jet quenching and signatures of a deconfined medium [4].

Subsequent measurements of jets in Pb+Pb collisions have improved the understanding of properties of quenched jets and the empirical features of the quenching mechanism [5–14]. Significant theoretical advances also occurred in this period, and while a complete description of jet quenching is not available, some models are capable of reproducing its key features and providing testable predictions. Measurements of the dijet asymmetry, $A_{\mathrm{J}} \equiv (p_{\mathrm{T}_1} - p_{\mathrm{T}_2})/(p_{\mathrm{T}_1} + p_{\mathrm{T}_2})$, where $p_{\mathrm{T}_1}$ and $p_{\mathrm{T}_2}$ are the transverse momenta of the jets with the highest and second highest $p_{\mathrm{T}}$ in the event, respectively, have been crucial in facilitating these developments. The experimental results demonstrate that the measured asymmetries in central collisions, where the geometric overlap of the colliding nuclei is almost complete, differ from those in $pp$ collisions more than is expected from detector-specific experimental effects [3,9,10]. However, such effects, in particular the resolution of the measured jet $p_{\mathrm{T}}$, must be corrected for in order for the measurement to be directly compared to theoretical calculations. Unfolding procedures have been applied to correct for such effects for single-jet measurements [6]; however, the dijet result requires a two-dimensional unfolding to account for migration in the $p_{\mathrm{T}}$ of each jet separately. The measurement reported here is the first unfolded Pb+Pb dijet measurement and as such can be directly compared to theoretical models.

This Letter presents a measurement of dijet $p_{\mathrm{T}}$ correlations in Pb+Pb and $pp$ collisions at a nucleon–nucleon centre-of-mass energy of 2.76 TeV performed with the ATLAS detector. Jets are reconstructed with the anti-$k_t$ algorithm with radius parameter values $R = 0.3$ and $R = 0.4$ [15]. The analysis is described mostly for the example of $R = 0.4$ jets. A background subtraction procedure is applied to account for the effects of the large underlying event (UE) present in Pb+Pb collisions on the measured jet kinematics. The momentum balance of the dijet system is expressed

* *E-mail address:* atlas.publications@cern.ch.

https://doi.org/10.1016/j.physletb.2017.09.078

by the variable $x_J \equiv p_{T_2}/p_{T_1}$. Measurements of the dijet yield normalised by the total number of jet pairs in a given $p_{T_1}$ interval, $(1/N)dN/dx_J$, are presented as a function of $x_J$ in intervals of $p_{T_1}$ and collision centrality. The results are obtained by first measuring the two-dimensional distribution, $(p_{T_1}, p_{T_2})$, and unfolding in the two-dimensional space. The binning in the $(p_{T_1}, p_{T_2})$ distribution is chosen such that the bins in the two-dimensional space correspond to fixed ranges of $x_J$, and the $(1/N)dN/dx_J$ results are obtained by projecting into these $x_J$ bins. The $(p_{T_1}, p_{T_2})$ distributions are less strongly correlated for jets reconstructed with a smaller value of $R$ due to the effects of parton radiation outside the jet cone, which makes them less suitable as a probe of medium-induced effects in Pb+Pb collisions. However, for smaller jet sizes the effect of the UE on the measurement is significantly reduced. It is therefore interesting to compare the results obtained using $R = 0.3$ and $R = 0.4$ jets, to see if the same features are visible.

## 2. Experimental set-up

The measurements presented in this Letter are performed using the ATLAS inner detector, calorimeter and trigger systems [16]. The inner detector provides measurements of charged-particle tracks over the range $|\eta| < 2.5$.[1] It is composed of silicon pixel detectors in the innermost layers, followed by silicon microstrip detectors and a straw-tube tracker, all immersed in a 2 T axial magnetic field provided by a solenoid. The minimum-bias trigger scintillators (MBTS) measure charged particles over $2.1 < |\eta| < 3.9$ using two planes of counters placed at $z = \pm 3.6$ m and provide timing measurements used in the event selection [17].

The ATLAS calorimeter system consists of a liquid argon (LAr) electromagnetic (EM) calorimeter ($|\eta| < 3.2$), a steel–scintillator sampling hadronic calorimeter ($|\eta| < 1.7$), a LAr hadronic calorimeter ($1.5 < |\eta| < 3.2$), and a forward calorimeter (FCal) ($3.2 < |\eta| < 4.9$). The hadronic calorimeter has three sampling layers longitudinal in shower depth and has a $\Delta\eta \times \Delta\phi$ granularity of $0.1 \times 0.1$ for $|\eta| < 2.5$ and $0.2 \times 0.2$ for $2.5 < |\eta| < 4.9$.[2] The EM calorimeters are longitudinally segmented in shower depth into three compartments following a pre-sampler layer ($|\eta| < 1.8$). The EM calorimeter has a granularity that varies with layer and pseudorapidity, but which is generally much finer than that of the hadronic calorimeter. The first layer has high $\eta$ granularity (between 0.003 and 0.006) that can be used to identify photons and electrons. The middle sampling layer, which typically has the largest energy deposit in EM showers, has a granularity of $0.025 \times 0.025$ over $|\eta| < 2.5$. A total transverse energy (TE) trigger is implemented by requiring a hardware-based determination of the total transverse energy in the calorimeter system, $E_T^{tot}$, to be above a threshold.

The zero-degree calorimeters (ZDCs) are located symmetrically at $z = \pm 140$ m and cover $|\eta| > 8.3$. In Pb+Pb collisions the ZDCs primarily measure "spectator" neutrons: neutrons that do not interact hadronically when the incident nuclei collide. A ZDC coincidence trigger is implemented by requiring the pulse height from each ZDC to be above a threshold set below the single-neutron peak.

In addition to the ZDC and TE hardware-based triggers, a software-based high-level trigger is used to further reduce the accepted event rate. This trigger applies a jet reconstruction procedure, including a UE subtraction, similar to that used in the offline analysis, which is described in Section 4.

## 3. Data and Monte Carlo samples

The Pb+Pb data used for these measurements were recorded in 2011 and obtained using a combination of jet and minimum-bias triggers. The minimum-bias trigger is defined by a logical OR of the TE trigger with a threshold of $E_T^{tot} = 50$ GeV and the ZDC coincidence trigger. The combined trigger is fully efficient in the range of centralities presented here. In the events selected by the ZDC coincidence trigger alone, at least one track is required to remove empty events. The jet trigger [18] first selects events satisfying the TE trigger with a threshold of $E_T^{tot} = 20$ GeV. A jet reconstruction procedure is then applied using the anti-$k_t$ algorithm with $R = 0.2$ and utilising a UE subtraction procedure similar to that used in the offline reconstruction described in Section 4. Events with at least one jet with $E_T > 20$ GeV at the electromagnetic scale [19] are selected by the jet trigger. The use of $R = 0.2$ for jets in the trigger, as opposed to the values of $R = 0.3$ and 0.4 applied in the measurement, is motivated by the need to define an algorithm that is robust against UE fluctuations, which grow with $R$. The effects of the different $R$ values on the trigger efficiency are discussed in Section 5. The minimum-bias trigger operated with a prescale of approximately 18 while no prescale was applied to the jet trigger. After accounting for these prescales, the recorded events correspond to integrated luminosities of 8 $\mu b^{-1}$ and 0.14 $nb^{-1}$ for the minimum-bias and jet-triggered samples, respectively.

Events are further subjected to criteria designed to remove non-collision background and inelastic electromagnetic interactions between the nuclei. Events are required to have a reconstructed primary vertex and have a timing difference of less than 5 ns between the times measured by the two MBTS planes. After the trigger and event selection criteria, the resulting data samples contain 53 and 14 million events in the minimum-bias and jet triggered samples, respectively. The average number of collisions per bunch-crossing in the Pb+Pb data sample was less than 0.001, and the effects of multiple collisions are neglected in the data analysis.

The centrality of the Pb+Pb collisions is characterised by the total transverse energy measured in the FCal modules, $\sum E_T^{FCal}$. The $\sum E_T^{FCal}$ distribution obtained in minimum-bias collisions is partitioned into separate ranges of $\sum E_T^{FCal}$ referred to as centrality classes [17,20,21]. Each class is defined by the fraction of the distribution contained by the interval, e.g. the 0–10% centrality class, which corresponds to the most central collisions, contains the 10% of minimum-bias events with the largest $\sum E_T^{FCal}$. The centrality boundaries used in this analysis are 0%, 10%, 20%, 30%, 40%, 60% and 80%.

The $pp$ data sample, recorded in 2013, was composed of events selected by a jet trigger and used a series of different $p_T$ thresholds each selected with a different prescale. The jet trigger is the same used in other ATLAS measurements in $pp$ collisions [18] and applies the anti-$k_t$ algorithm with $R = 0.4$. The events are further required to contain at least one primary reconstructed vertex. The average number of $pp$ collisions per bunch-crossing varied between 0.3 and 0.6 during data taking. The sample corresponds to a luminosity of 4.0 $pb^{-1}$.

The impact of experimental effects on the measurement is evaluated using the GEANT4-simulated detector response [22,23] in a Monte Carlo (MC) sample of $pp$ hard-scattering events. Dijet events at $\sqrt{s} = 2.76$ TeV are generated using PYTHIA version 6.423 [24] with parameter values chosen according to the AUET2B tune [25] using the CTEQ6L1 parton distribution function (PDF) set [26]. To

[1] ATLAS uses a right-handed coordinate system with its origin at the nominal interaction point (IP) in the centre of the detector and the $z$-axis along the beam pipe. The $x$-axis points from the IP to the centre of the LHC ring, and the $y$-axis points upward. Cylindrical coordinates $(r, \phi)$ are used in the transverse plane, $\phi$ being the azimuthal angle around the beam pipe. The pseudorapidity is defined in terms of the polar angle $\theta$ as $\eta = -\ln\tan(\theta/2)$.

[2] An exception is the third sampling layer, which has a segmentation of $0.2 \times 0.1$ up to $|\eta| = 1.7$.

fully populate the kinematic range considered in the measurement, hard-scattering events are generated for separate intervals of $\hat{p_T}$, the transverse momentum of outgoing partons in the $2 \to 2$ hard-scattering, and combined using weights proportional to their respective cross sections. Separate samples are generated for the Pb+Pb and $pp$ analyses, with the simulated detector conditions chosen to match those present during the recording of the respective data samples. In the $pp$ data sample, the contribution of additional collisions in the same bunch crossing (pile-up) is accounted for by overlaying minimum-bias $pp$ collisions produced at the same rate as in the data, generated by Pythia version 8.160 [27] using the A2 [28] tune with CT10 PDF set [29]. In the Pb+Pb sample, the UE contribution to the detector signal is accounted for by overlaying the simulated events with minimum-bias Pb+Pb data. The vertex position of each simulated event is selected to match the data event that is overlaid. Through this procedure the MC sample contains contributions from underlying-event fluctuations and harmonic flow that match those present in the data. The combined signal is then reconstructed using the same procedure as is applied to the data. So-called *truth jets* are defined by applying the anti-$k_t$ algorithm with $R = 0.3$ and $R = 0.4$ to stable particles in the MC event generator's output, defined as those with a proper lifetime greater than 10 ps, but excluding muons and neutrinos, which do not leave significant energy deposits in the calorimeter.

The detector's response to quenched jets is studied with an additional sample using Pyquen [30]. This event generator applies medium-induced energy loss to parton showers produced by Pythia. It is used to generate a sample of jets with fragmentation functions that differ from those in the nominal Pythia sample in a fashion consistent with measurements of fragmentation functions in quenched jets [11–13].

## 4. Jet reconstruction

The procedure used to reconstruct jets in heavy-ion collisions is described in detail in Ref. [5] and is briefly summarised here. First, energy deposits in the calorimeter cells are assembled into $\Delta\eta \times \Delta\phi = 0.1 \times \frac{\pi}{32}$ logical towers. Jets are formed from the towers by applying the anti-$k_t$ algorithm [15] as implemented in the `FastJet` software package [31].

An estimate of the UE contribution to each tower within the jet is performed on an event-by-event basis by estimating the transverse energy density, $\rho(\eta, \phi)$. Global azimuthal modulation in the UE arises due to the physics of flow and is traditionally described in terms of the Fourier expansion of the $\phi$ dependence of the transverse energy density. In the subtraction procedure, the UE estimate is assigned a $\phi$ dependence using the measured magnitudes and phases of the modulation:

$$\rho(\eta, \phi) = \overline{\rho}(\eta) \times \left(1 + 2\sum_n v_n \cos[n(\phi - \Psi_n)]\right), \quad (1)$$

where $v_n$ and $\Psi_n$ are the magnitudes and phases of the harmonic modulation, respectively, and $\overline{\rho}(\eta)$ is the average transverse energy density measured from energy deposits in the calorimeter as a function of $\eta$. In Ref. [5], only the second-order harmonic modulation ($n = 2$) was considered, but in this measurement the procedure has been extended to account for $n = 3$ and 4 harmonic modulations as well. The subtraction is applied to each tower within the jet. The quantities in Eq. (1) may be biased if the energy in a jet is included in their calculation, which results in an over-subtraction of the average UE contribution to the jet energy or incomplete removal of the harmonic modulation. To mitigate such effects, the contribution from jets is excluded from the estimate of the background. The typical background energy subtracted from the jets varies from a few GeV in peripheral collisions to 150 GeV in the most central collisions.

A calibration factor, derived from MC studies, is then applied after the subtraction to account for the non-compensating hadronic response. A final *in situ* calibration is applied to account for known differences in detector response between data and the MC sample used to derive the initial calibration [32]. This calibration is derived in 8 TeV $pp$ data and adapted to the different beam energy and pile-up conditions relevant for the samples considered here. It uses the balance between jet pairs in different $\eta$ regions of the detector to provide an evaluation of the relative response to jets as a function of $\eta$. It subsequently uses jets recoiling against objects with an independently-determined energy scale such as $Z$ bosons or photons to provide constraints on the absolute energy measurement.

## 5. Data analysis

In this analysis, jet pairs are formed from the two highest-$p_T$ jets in the event with $p_T > 25$ GeV and $|\eta| < 2.1$. The pair is required to have $\Delta\phi > 7\pi/8$, where $\Delta\phi \equiv |\phi_1 - \phi_2|$. For events selected by a jet trigger, the leading jet is required to match a jet identified by the trigger algorithm responsible for selecting the jet. The two-dimensional $(p_{T_1}, p_{T_2})$ distributions obtained from different triggered samples are combined such that intervals of $p_{T_1}$ are populated by a single trigger. In the $pp$ data analysis, the trigger with the most events that is more than 99% efficient for selecting a jet with $p_T > p_{T_1}$ is used, with the reciprocal of the luminosity for the respective trigger samples used as a weight.

The Pb+Pb jet trigger efficiency has a broad turn-on as a function of $p_T$ since the trigger jets are identified using $R = 0.2$ and have no energy scale calibration applied. This effect is the strongest in central collisions where the UE fluctuations are the largest and further weaken the correlation between jets reconstructed with different values of $R$. In the most central collisions, the single-jet-trigger efficiency does not reach a plateau until $p_T \sim 90$ GeV. The jet-triggered sample is used where the efficiency is found to be greater than 97%, which occurs at a $p_T$ of approximately 85 GeV in the most central collisions. A trigger efficiency correction is applied in the region where there is an inefficiency.

In addition to the dijet signal, the measured $(p_{T_1}, p_{T_2})$ distribution receives contributions from so-called *combinatoric* jet pairs. Such pairs arise when two jets, which are not from the same hard-scattering process, fulfil the pair requirements through random association. Jets forming such pairs may originate from independent hard scatterings or from upward UE fluctuations identified as jets, referred to as UE jets. The rate for such occurrences is highest in the most central collisions, and the reduction in the true sub-leading jet $p_T$ due to quenching effects further enhances the likelihood of forming a combinatoric pair.

The shape of the $\Delta\phi$ distribution for the combinatoric jet pairs is influenced by the harmonic flow. Since the jet $p_T$ spectrum falls steeply, the jets most likely to be measured at a given $p_T$ value are those lying on top of larger-than-average UE. If the effects of the modulation of the UE are not fully accounted for in the background subtraction, more jets would be observed at angles corresponding to the flow maxima ($\phi \sim \Psi_n$). Thus combinatoric jet pairs, without any underlying angular correlation, are expected to acquire a modulation to their $\Delta\phi$ distribution determined by the dominant flow harmonics [33]. Although the second-, third- and fourth-order harmonic modulations are considered event-by-event in the jet reconstruction procedure described in Section 4, only the effects of the second-order modulation on the $\Delta\phi$ distribution are observed to be completely removed. The residual effects are an indication that the method of estimating the modulation of the UE under-

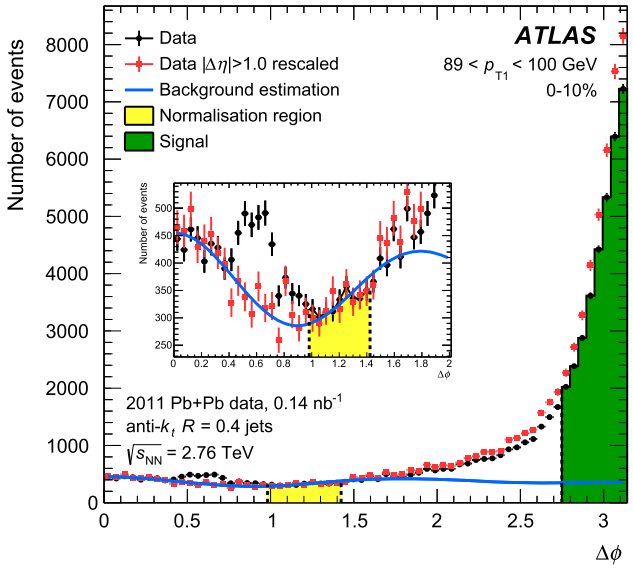


**Fig. 1.** The $\Delta\phi$ distribution for $R = 0.4$ jet pairs with $89 < p_{T_1} < 100$ GeV in the 0–10% centrality interval. The distribution for all jet pairs is indicated by the black circles. The combinatoric contribution given by Eq. (2) is shown as a blue line. The ranges of $\Delta\phi$ used to fix the value of $Y$ and to define the signal region ($\Delta\phi > \frac{7\pi}{8}$) are indicated by yellow and green shaded regions, respectively. The parameters $c_3$ and $c_4$ are obtained by fitting the $\Delta\phi$ distribution for jet pairs with $|\Delta\eta| > 1$ in the region $0 < \Delta\phi < \frac{\pi}{2}$, which is indicated by the red squares (scaled to match the black circles in the yellow region for presentation purposes). The error bars denote statistical errors. (For interpretation of the references to colour in this figure, the reader is referred to the web version of this article.)

neath the jet is less accurate for the higher-order harmonics than for $n = 2$.

To account for the residual modulation, the combinatoric contribution is assumed to be of the form:

$$C(\Delta\phi) = Y(1 + 2c_3 \cos 3\Delta\phi + 2c_4 \cos 4\Delta\phi)\,. \tag{2}$$

The $c_3$ and $c_4$ values are determined by fitting the $\Delta\phi$ distributions over the range $0 < \Delta\phi < \pi/2$ where the real dijet contribution is expected to be small. The region $0 < \Delta\phi \lesssim 0.8$ is also expected to receive real dijet contributions arising from parton radiation which results in pairs of jets at nearby angles. To remove this contribution, the fit to obtain $c_3$ and $c_4$ is performed only using jet pairs with a separation of $|\Delta\eta| > 1$. Once $c_3$ and $c_4$ are obtained, the $\Delta\phi$ distribution without this $|\Delta\eta|$ requirement is integrated over the range $1 < \Delta\phi < 1.4$ to obtain $Y$. This procedure is performed separately in each $(p_{T_1}, p_{T_2})$ interval. In intervals where the $c_3$ and $c_4$ are found to not be statistically significant their values are taken to be zero. The expected combinatorial contribution, $B$, in the signal region is obtained by integrating $C(\Delta\phi)$ from $7\pi/8$ to $\pi$.

The $\Delta\phi$ distribution of jet pairs is shown in Fig. 1 for pairs with $89 < p_{T_1} < 100$ GeV in the 0–10% centrality interval. Also shown is the $\Delta\phi$ distribution obtained from such jet pairs with $|\Delta\eta| > 1$, which is fitted to obtain $c_3$ and $c_4$. The background subtraction is most significant in central collisions, where the fraction subtracted from the total yield in the signal region is as large as 10% for small $x_J$ and is less than 1% for $x_J$ values greater than 0.5. The background contribution in more peripheral collisions is less than 1% for all values of $x_J$. This background subtraction is not applied in the $pp$ data because the pile-up is small.

The presence of combinatoric jet pairs also reduces the efficiency for genuine pairs. The measured inclusive jet spectrum is used to estimate the likelihood that another jet in the event, uncorrelated with the dijet system, is measured with a transverse momentum greater than $p_{T_2}$. For the 40–60% and 60–80% centrality intervals the effect is negligible. In the 0–10% centrality bin the efficiency is approximately 0.9 for $p_{T_2} = 25$ GeV and increases with $p_{T_2}$, reaching unity at 45 GeV. The effects of the combinatoric jet pairs are accounted for by first subtracting the estimated background and then correcting for the efficiency, $\varepsilon$, in each $(p_{T_1}, p_{T_2})$ bin. The number of jet pairs corrected for such effects is defined to be:

$$N^{\text{corr}} = \frac{1}{\varepsilon}\left(N^{\text{raw}} - B\right),$$

where $N^{\text{raw}}$ is the number of jet pairs after correcting for trigger efficiency and luminosity/prescale weighting as described above.

In a given event, the $p_T$ resolution may result in the jet with the highest true $p_T$ being measured with the second highest $p_T$ and vice-versa. To properly account for such migration effects, $(p_{T_1}, p_{T_2})$ distributions are symmetrised prior to the unfolding by apportioning half of the yield in a given $(p_{T_1}, p_{T_2})$ bin, after combinatoric subtraction, to the bin related to the original by $p_{T_1} \leftrightarrow p_{T_2}$. The two-dimensional distributions after symmetrisation are shown in Fig. 2 for central and peripheral Pb+Pb collisions and for $pp$ collisions. The choice of binning in $(p_{T_1}, p_{T_2})$ is motivated by the mapping to the $x_J$ variable, and is described in more detail in the following section.

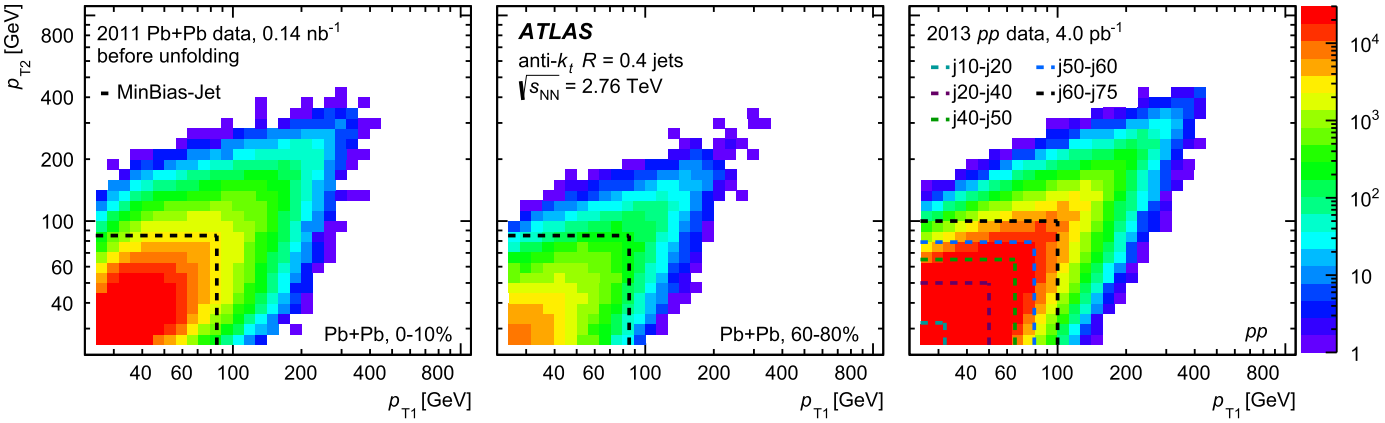


**Fig. 2.** The two-dimensional $(p_{T_1}, p_{T_2})$ distributions after correction and symmetrisation for Pb+Pb data in the 0–10% (left) and 60–80% (centre) centrality bins and for $pp$ data (right) for $R = 0.4$ jets. The dashed lines indicate the boundaries used in selecting the different triggers. The Pb+Pb data distributions have their combinatoric contribution subtracted.

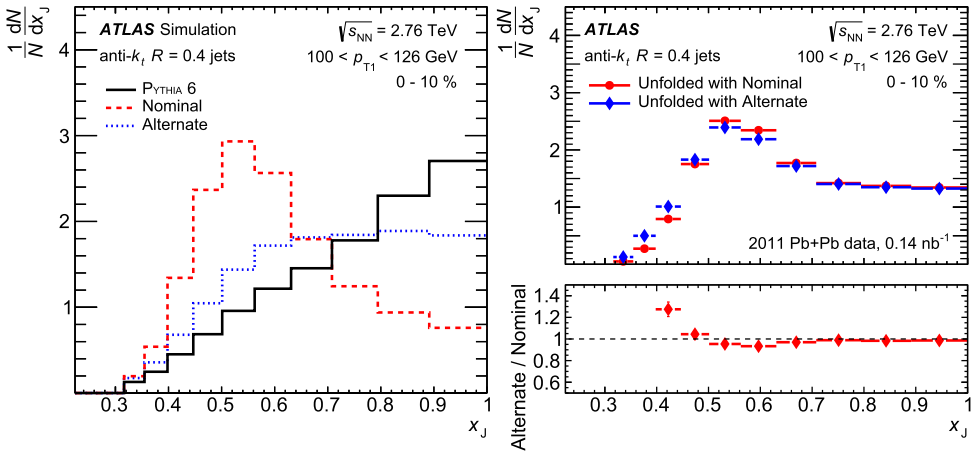


**Fig. 3.** Left: the $(1/N)\mathrm{d}N/\mathrm{d}x_\mathrm{J}$ distributions used as priors in the unfolding of the $R = 0.4$ jets for the nominal (dashed red) and alternate variation (dotted blue) for the $100 < p_{\mathrm{T}_1} < 126$ GeV and 0–10% centrality interval. The same distribution obtained from the PYTHIA MC sample is shown in solid black. Right: unfolded $(1/N)\mathrm{d}N/\mathrm{d}x_\mathrm{J}$ distributions from data for the same $p_{\mathrm{T}_1}$ and centrality ranges using the nominal (red circles) and alternate (blue diamonds) priors shown in the left panel. The ratio of nominal to alternate is shown in the bottom panel. In the bottom panel on the right the first two bins are off scale with bins centres of $x_\mathrm{J} = 0.34$ and 0.38 and bins contents of 2.49 and 1.82, respectively. Statistical errors are not shown. (For interpretation of the references to colour in this figure, the reader is referred to the web version of this article.)

## 6. Unfolding

The calorimetric response to jets is evaluated in the MC sample by matching truth and reconstructed jets; the nearest reconstructed and truth jets within $\Delta R = \sqrt{(\Delta\eta)^2 + (\Delta\phi)^2}$ of 0.3 are considered to be a match. The same requirement is applied in both the $R = 0.3$ and $R = 0.4$ versions of the analysis. The response is typically characterised in terms of the jet energy scale (JES) and jet energy resolution (JER). These quantities describe the mean and width of the $p_\mathrm{T}^\mathrm{reco}$ distributions at fixed $p_\mathrm{T}^\mathrm{truth}$, expressed as a fraction of $p_\mathrm{T}^\mathrm{truth}$. Generally, the mean of $p_\mathrm{T}^\mathrm{reco}$ differs from $p_\mathrm{T}^\mathrm{truth}$ by less than a percent, independent of $p_\mathrm{T}^\mathrm{truth}$ and centrality. This indicates that the subtraction of the average UE contribution to the jet energy is under good experimental control. The JER receives contributions both from the response of the calorimeter and from local UE fluctuations about the mean in the region of the jet. The latter contribution dominates at low $p_\mathrm{T}$ with the resolution as large as 40% at $p_\mathrm{T} \simeq 30$ GeV in the most central collisions. At the same $p_\mathrm{T}$, the JER is only 20% in peripheral collisions, similar to that in $pp$ collisions. At larger $p_\mathrm{T}$ values the relative contribution of the UE fluctuations to the jet $p_\mathrm{T}$ diminishes, and the JER is dominated by detector effects, reaching a constant, centrality-independent value of 8% for $p_\mathrm{T} > 300$ GeV.

The migration in the two-dimensional $(p_{\mathrm{T}_1}, p_{\mathrm{T}_2})$ distribution is accounted for by applying a two-dimensional Bayesian unfolding to the data [34,35]. This procedure utilizes a response matrix obtained by applying the same pair selections to the truth jets in MC simulation as in the data analysis (except the trigger requirement) and recording the values of $p_{\mathrm{T}_1}^\mathrm{truth}$ and $p_{\mathrm{T}_2}^\mathrm{truth}$ and the transverse momenta of the corresponding reconstructed jets $p_{\mathrm{T}_1}^\mathrm{reco}$ and $p_{\mathrm{T}_2}^\mathrm{reco}$. The matched reconstructed jets are not required to have the highest $p_\mathrm{T}$ in the event, but are subject to all other requirements applied to the data and truth jets. The response matrix is populated symmetrically in both truth and reconstructed $p_\mathrm{T}$. The full four-dimensional response behaves similarly to the factorised product of separate single-jet response distributions, and the migration effects can be understood in terms of the above discussion. While this provides intuition for the nature of the unfolding problem, such a factorisation is not explicitly assumed, and any correlations between the response of the two jets are accounted for in the procedure.

After unfolding, the leading/sub-leading distinction is restored by reflecting the distribution over the line $p_{\mathrm{T}_1} = p_{\mathrm{T}_2}$: for each bin with $p_{\mathrm{T}_2} > p_{\mathrm{T}_1}$ the yield is moved to the corresponding bin with $p_{\mathrm{T}_2} < p_{\mathrm{T}_1}$. The bins along the diagonal, e.g. those containing pairs with $p_{\mathrm{T}_2} = p_{\mathrm{T}_1}$, are not affected by this procedure. The two-dimensional distribution is constructed using binning along each axis such that the upper edge of the $i$th bin obeys,

$$p_{\mathrm{T}\,i} = p_{\mathrm{T}\,0}\,\alpha^i\,, \quad \alpha = \left(\frac{p_{\mathrm{T}\,N}}{p_{\mathrm{T}\,0}}\right)^{1/N}\,,$$

where $N$ is the total number of bins and $p_{\mathrm{T}\,0}$ and $p_{\mathrm{T}\,N}$ are the minimum and maximum bin edges covered by the binning, respectively. As a consequence, the bins are of the same size when plotted with logarithmic axes. With these choices of binning, the range of $x_\mathrm{J}$ values in any given $(p_{\mathrm{T}_1}, p_{\mathrm{T}_2})$ bin is fully contained within two adjacent $x_\mathrm{J}$ bins, which have boundaries at $x_{\mathrm{J}\,i} = \alpha^{i-N}$. In this analysis, half of the yield in each $(p_{\mathrm{T}_1}, p_{\mathrm{T}_2})$ bin is apportioned to each of the $x_\mathrm{J}$ bins. The exceptions are the bins along the diagonal. These bins contribute solely to the $x_\mathrm{J}$ bin with bin edges $(\alpha^{-1}, 1)$. The effects of such a mapping on the $x_\mathrm{J}$ distribution are studied and found to not significantly distort the shape of the distribution for a variety of input $x_\mathrm{J}$ distributions.

The Bayesian unfolding method is an iterative procedure that requires both a choice in a number of iterations, $n_\mathrm{iter}$, and assumption of a prior for the underlying true distribution. An increase in $n_\mathrm{iter}$ reduces sensitivity to the choice of prior but may amplify statistical fluctuations that are already present in the input distribution. As PYTHIA does not include the effects of jet quenching, the $x_\mathrm{J}$ distributions obtained from the MC sample are not expected to be optimal choices for the prior. In particular, the $x_\mathrm{J}$ distributions in PYTHIA increase monotonically with $x_\mathrm{J}$, whereas the distributions in the data become flatter and develop a peak near $x_\mathrm{J} \sim 0.5$ in lower $p_{\mathrm{T}_1}$ intervals and in the most central collisions. The $(p_{\mathrm{T}_1}, p_{\mathrm{T}_2})$ distributions from PYTHIA are reweighted in a centrality-dependent way to obtain features that qualitatively match those present in the data.

The effects of the reweighting procedure are shown in the left panel of Fig. 3 in the $100 < p_{\mathrm{T}_1} < 126$ GeV range and 0–10% centrality interval, where the largest difference between the data and PYTHIA is observed. The "nominal" distribution, or the reweighted distribution, is used as the prior in the unfolding of the data. An

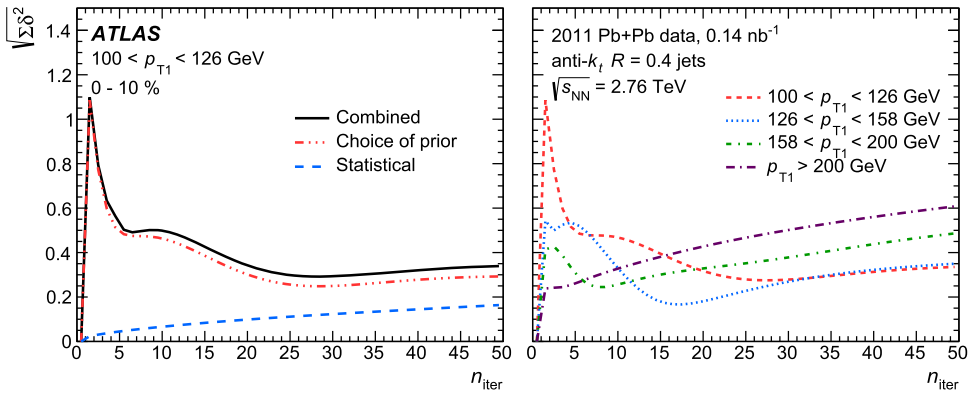


**Fig. 4.** Uncertainties sensitive to the number of iterations in the unfolding procedure as a function of $n_{\text{iter}}$ for the 0–10% centrality interval for $R = 0.4$ jets. Left: The combination (solid black) of the unfolding (dashed red) and statistical (dotted blue) uncertainty, $\sqrt{\Sigma\delta^2}$ for the $100 < p_{T_1} < 126$ GeV interval. Right: The combined uncertainty for each $p_{T_1}$ interval considered in the measurement. (For interpretation of the references to colour in this figure, the reader is referred to the web version of this article.)

"alternate" reweighting is also shown, which has a shape significantly different from the nominal, but does not increase as much as the Pythia distribution. The features in the data are observed to be robust with respect to the choice of prior for a broad set of reweighting functions. The systematic uncertainty due to the choice of prior is estimated by comparing the results of the unfoldings using the "nominal" and "alternate" $x_{\text{J}}$ distributions. The results of applying unfoldings with these two choices of priors are shown in the right panels of Fig. 3 for the same $p_{T_1}$ and centrality selection.

An alternative study is performed in the MC sample to validate the estimation of this uncertainty. The "alternate" reweighting is applied to obtain input truth and reconstructed distributions in which no peak structure is present. The reconstructed distribution is then unfolded using the *nominal* prior. The unfolded distribution does not develop the strong peak present in the nominal prior. The differences between the unfolded result and the input truth distribution are similar to the uncertainty obtained by varying the prior used to unfold the data.

The value of $n_{\text{iter}}$ is selected separately in each centrality interval by examining the uncertainty, $\sqrt{\Sigma\delta^2}$, in $(1/N)\mathrm{d}N/\mathrm{d}x_{\text{J}}$ after unfolding considering statistical uncertainties and systematic uncertainties attributed to the unfolding procedure,

$$\delta^2 = \delta^2_{\text{stat}} + \delta^2_{\text{prior}},$$

and summing over all $x_{\text{J}}$ bins. Here $\delta_{\text{prior}}$ is the uncertainty due to the choice of prior, obtained using the procedure described above. The statistical uncertainties are evaluated using a pseudo-experiment technique. Stochastic variations of the data are generated based on its statistical uncertainty and each variation is unfolded and projected into $x_{\text{J}}$. The statistical covariance of the set is taken as the statistical uncertainty. An additional covariance is obtained from applying the pseudo-experiment procedure to the response matrix and combined with that obtained from applying the procedure to the data. The $\delta^2_{\text{stat}}$ for each $x_{\text{J}}$ bin is taken to be the diagonal element of the resulting covariance matrix. The statistical covariance matrices exhibit similar trends across all $p_{T_1}$ and centrality ranges. Nearby $x_{\text{J}}$ bins show a strong positive correlation that diminishes for bins separated in $x_{\text{J}}$, and is expected from the effects of the procedures for unfolding and mapping to $x_{\text{J}}$. Bins well separated in $x_{\text{J}}$ show an anti-correlation attributable to the normalisation of $(1/N)\mathrm{d}N/\mathrm{d}x_{\text{J}}$.

The left panel of Fig. 4 shows $\sqrt{\Sigma\delta^2}$ as a function of $n_{\text{iter}}$ along with its various contributions for the $100 < p_{T_1} < 126$ GeV range and 0–10% centrality interval. Since the unfolding is performed in two dimensions, the value of $n_{\text{iter}}$ cannot be chosen separately for each range of $p_{T_1}$. At higher values of $p_{T_1}$ the effects of the unfolding are smaller while the effects of the statistical fluctuations can be more severe. The right panel of Fig. 4 shows the total $\sqrt{\Sigma\delta^2}$ for each range of $p_{T_1}$ considered in the measurement along with the total combined over all $p_{T_1}$ ranges. The value of $n_{\text{iter}}$ for each centrality bin and $R$ value is chosen by considering the $n_{\text{iter}}$ dependence of $\sqrt{\Sigma\delta^2}$ for each $p_{T_1}$ bin and selecting a value that maintains comparable uncertainties across all $p_{T_1}$ ranges. The more central bins require the most iterations, resulting from the larger jet energy resolution in these events. The number of iterations for $R = 0.4$ jets is at most 20 for 0–10% centrality and at the least 6 for 60–80% centrality. The $\sqrt{\Sigma\delta^2}$ distributions for $R = 0.3$ jets show behaviour similar to those for $R = 0.4$ jets in the same centrality bin.

It is possible for a third jet present in the event to be reconstructed as the jet with the second highest $p_{\text{T}}$ through the experimental resolution. As a check to study the impact of such effects on the measurement, an alternative response matrix is constructed where no $\Delta R$ matching is required between the truth and reconstructed jets. A weighting is applied such that the $p_{\text{T}}$ distribution of the reconstructed third jet matches that observed in the data. Differences between the unfolded distributions obtained with this response matrix and the nominal one are observed to be small and well within the systematic uncertainty associated with the unfolding procedure.

The $(1/N)\mathrm{d}N/\mathrm{d}x_{\text{J}}$ distributions before and after unfolding are shown in Fig. 5 for central and peripheral Pb+Pb collisions and for $pp$ collisions for jet pairs with $100 < p_{T_1} < 126$ GeV. The systematic uncertainties indicated contain all of the contributions to the total systematic uncertainty described in Section 7. In the $pp$ and 60–80% centrality interval, the resolution effects before unfolding reduce the sharpness of the peak near $x_{\text{J}} \sim 1$. In the case of the 0–10% centrality interval, the effect is to smear out the peak near $x_{\text{J}} \sim 0.5$. The lowest $x_{\text{J}}$ bins exhibit instability in the unfolding procedure due to the MC sample having too few events in this region. However, including this range in the unfolding improves the stability of the adjacent $x_{\text{J}}$ bins. Thus, after unfolding, only the range $0.32 < x_{\text{J}} < 1$ is reported in the results even though pairs with $p_{T_2} > 25$ GeV are included in the measurement.

## 7. Systematic uncertainties

Systematic uncertainties attributed to the response matrix used in the unfolding arise due to uncertainties in the JES and JER. To account for these effects, new response matrices are constructed with a systematically varied relationship between the truth and

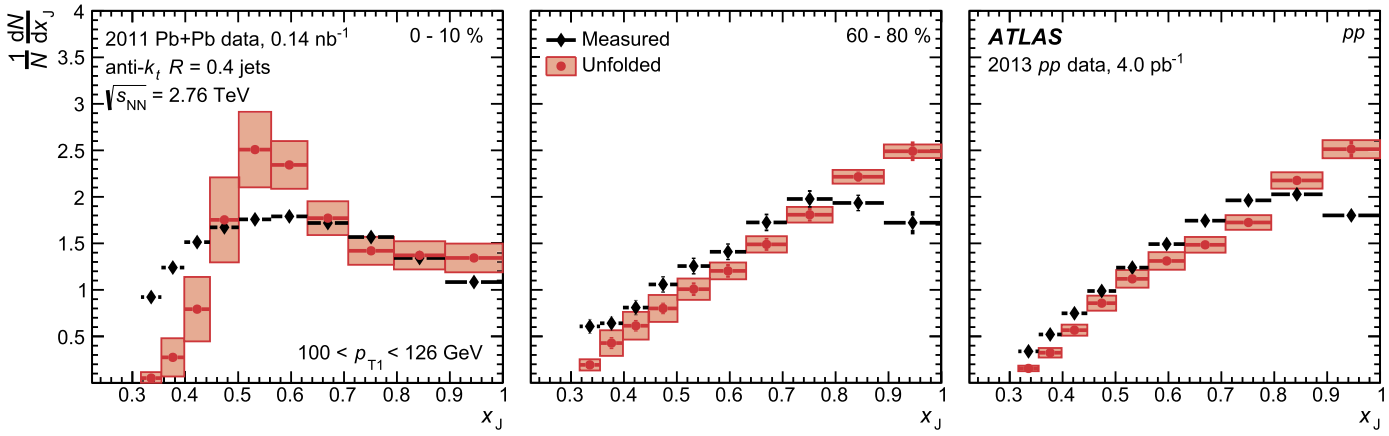


**Fig. 5.** The $(1/N)\mathrm{d}N/\mathrm{d}x_\mathrm{J}$ distributions for $R = 0.4$ jets before (black) and after (red) unfolding for the $100 < p_{\mathrm{T}_1} < 126$ GeV interval for the Pb+Pb 0–10% (left) and Pb+Pb 60–80% (middle) centrality ranges and for $pp$ collisions (right). Statistical uncertainties are indicated by vertical error bars (not visible in most cases). Systematic uncertainties in the unfolded result are indicated by the red shaded boxes. (For interpretation of the references to colour in this figure, the reader is referred to the web version of this article.)

reconstructed jet kinematics. The data are then unfolded using the new response and the result is compared with the nominal.

In the $pp$ data analysis, the JES uncertainty is described by a set of 11 independent nuisance parameters; these include effects from uncertainties derived through the *in situ* calibration [32]. In the MC sample used to determine the calibration, the calorimetric response to jets initiated by the fragmentation of quarks and gluons is observed to differ. Potential inaccuracies in the MC sample describing both this flavour-dependent response and the relative abundances of quark and gluon jets are accounted for using separate nuisance parameters. A source of uncertainty related to the adaptation of the *in situ* calibration derived at $\sqrt{s} = 8$ TeV to 2.76 TeV data is also included.

In the Pb+Pb data analysis, two additional uncertainties in the JES are considered. The first accounts for differences between the detector operating conditions in the Pb+Pb and $pp$ data, which were recorded in 2011 and 2013, respectively. This is derived by using charged-particle tracks reconstructed in the inner detector to provide an independent check on the JES, which only uses information from the calorimeter. For each jet, all reconstructed tracks within $\Delta R < 0.4$ and having $p_{\mathrm{T}}^{\mathrm{trk}} > 2$ GeV, are matched to the jet and the scalar sum of the track transverse momenta is evaluated. The ratio of this sum to the jet's $p_{\mathrm{T}}$ is evaluated both in data and in the MC sample, and a double ratio of the two quantities is formed. The double ratio obtained in peripheral Pb+Pb data is compared with that in $pp$ data. The precision of the comparison is limited by having too few events in the peripheral Pb+Pb data and at high jet $p_{\mathrm{T}}$, and a $p_{\mathrm{T}}$- and $\eta$-independent uncertainty of 1.46% is assigned to account for potential differences.

The second additional uncertainty is a centrality-dependent JES uncertainty to account for potential differences in the detector response to quenched jets. This is estimated by comparing the detector response evaluated in the Pythia and Pyquen MC samples. This estimate is checked in data using a track-based study similar to the one described above, but comparing central and peripheral Pb+Pb collisions and accounting for the measured variation of the fragmentation function with centrality [11–13]. An uncertainty of up to 1% in the most central collisions and decreasing linearly with centrality percentile to 0% in the 60–80% centrality class is assigned.

The uncertainty attributed to the JER is obtained by adding Gaussian fluctuations to each reconstructed jet $p_{\mathrm{T}}$ value when populating the response matrix. The magnitude of this uncertainty is fixed by a comparison of the data and MC descriptions of the JER in 8 TeV data [36]. Since the MC sample is constructed using the data overlay procedure, it is expected that the centrality dependence of the JER should be well described in the MC sample. This is checked by studying the distribution of UE fluctuations using random, jet-sized groups of calorimeter towers in Pb+Pb data. The standard deviations of these distributions describe the typical UE contribution beneath a jet. The centrality dependence of the UE fluctuations is compared to that of the JER in the MC sample, and a systematic uncertainty is included to account for the observed differences. As expected, these differences are much smaller than the centrality-independent contribution to the JER uncertainty.

The data-driven estimates of the JES and JER uncertainties described above are derived using $R = 0.4$ jets. Additional uncertainties are included in the $R = 0.3$ jet measurement to account for potential differences between data and the MC sample in the relative energy scale of $R = 0.3$ jets with respect to $R = 0.4$ jets. These uncertainties are estimated from a study that matched jets reconstructed with the two $R$ values and compared the means of the $p_{\mathrm{T}}^{R=0.3}/p_{\mathrm{T}}^{R=0.4}$ distributions in data and the MC sample. Differences may arise between the data and MC sample from differences in the calorimetric response or because the jets in the two samples have different internal structure. The contribution of the latter is constrained by using existing jet shape measurements [37]. An uncertainty in the energy scale is applied to account for residual differences, which are 1.5% at the lowest $p_{\mathrm{T}}$ and decrease sharply as a function of $p_{\mathrm{T}}$ to a limiting value of 0.3% at high $p_{\mathrm{T}}$. A similar study comparing the variances of the $p_{\mathrm{T}}^{R=0.3}/p_{\mathrm{T}}^{R=0.4}$ distributions is used to constrain the uncertainty in the relative resolution. This uncertainty is applied in the $R = 0.3$ jet measurement in the same fashion as the other JER uncertainties described above. Although larger than the centrality-dependent contribution, it is also much smaller than the centrality-independent contribution.

As the response matrix is sparsely populated (containing $40^4$ bins), statistical fluctuations could introduce instabilities in the unfolding. To evaluate the sensitivity to such effects, along with any other defects in the response, a new response matrix is constructed as a factorised product of single-jet response distributions, i.e. assuming the responses in $p_{\mathrm{T}_1}$ and $p_{\mathrm{T}_2}$ are independent. The data are unfolded using this new response and the differences between the unfolded distributions are taken as a systematic uncertainty. Systematic uncertainties in the unfolding due to the choice of prior are estimated as described in the previous section and are also included.

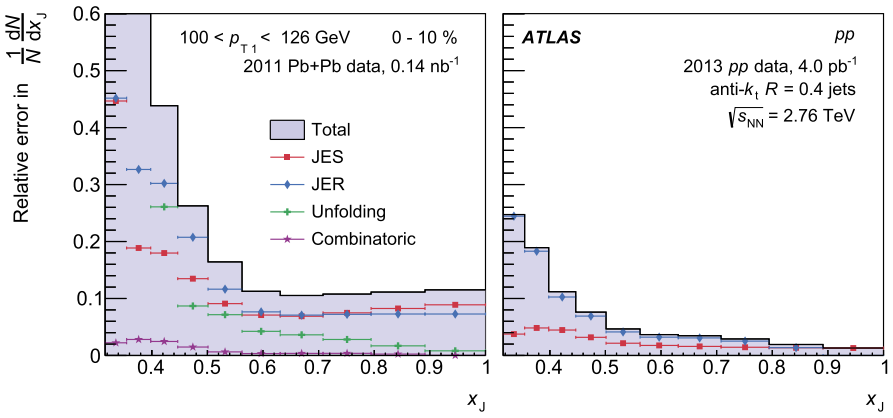


**Fig. 6.** The total systematic uncertainty and its various components for $100 < p_{T_1} < 126$ GeV for $R = 0.4$ jets in Pb+Pb collisions with 0–10% centrality (left) and $pp$ collisions (right). In the figure on the left the first two bins are off scale with bins centres of $x_J = 0.34$ and 0.38 and bins contents of 1.25 and 0.75, respectively.

Uncertainties due to the correction for the combinatoric effects described in Section 5 affect the number of jet pairs before the unfolding and are thus included as additional contributions to the previously described statistical uncertainties in the data. These include statistical uncertainties in $\varepsilon$ and the uncertainties in the values of the fit parameters $c_3$ and $c_4$, accounting for their covariance. Uncertainties in the normalisation are estimated by varying the region of $\Delta\phi$ used to estimate $Y$ from 1.0–1.4 to 1.1–1.5. The uncertainty due to this correction is smaller than the other uncertainties in all $p_T$ and centrality bins, and is only greater than 5% at values of $x_J < 0.4$. This correction was not applied to the $pp$ data so there is no corresponding systematic uncertainty.

The breakdown of different contributions to the total systematic uncertainty is shown in the $100 < p_{T_1} < 126$ GeV range for the 0–10% centrality interval and for $pp$ collisions in Fig. 6. Each contribution to the uncertainty, and thus the total uncertainty, tends to decrease with increasing $x_J$. The total uncertainty at $x_J \sim 1$ reaches approximately 12% in most $p_{T_1}$ and centrality bins in the Pb+Pb data. For $x_J < 0.4$, the relative uncertainty becomes large, but this region represents only a small contribution to the total $(1/N)dN/dx_J$ distribution. The JER uncertainty is the largest contribution. In the Pb+Pb data it reaches values of approximately 10% and 15% at $x_J \sim 1$ and $x_J = 0.5$, respectively. The JES contributions are the second largest contribution to the uncertainties, typically between 5% and 10%. In the most central bins the unfolding uncertainty can become as large as the JES contribution. The contributions to the uncertainty in the other centrality intervals and in the $pp$ data follow trends similar to those described for the 0–10% centrality interval, but the magnitudes are smaller in more peripheral collisions. In the $pp$ data they are typically smaller by a factor of two compared to the 0–10% Pb+Pb data. The uncertainties for the $R = 0.3$ result follow the same trends as those for the $R = 0.4$ result but are slightly larger due to the two additional sources included in that measurement to describe the relative energy scale and resolution between the two $R$ values.

## 8. Results

The unfolded $(1/N)dN/dx_J$ distribution in $pp$ collisions for $100 < p_{T_1} < 126$ GeV is shown in Fig. 7. Also shown are the corresponding distributions obtained from the Pythia 6 sample used in the MC studies and also from Pythia 8 using the AU2 tune and Herwig++ [38] with the UE-EE-3 [39] tune. An additional sample, referred to as Powheg+Pythia 8 is generated using Powheg-Box 2.0 [40–42], which is accurate to next-to-leading order in perturbative QCD, and interfaced with Pythia 8 to provide a description of the parton shower and hadronisation. All samples used the

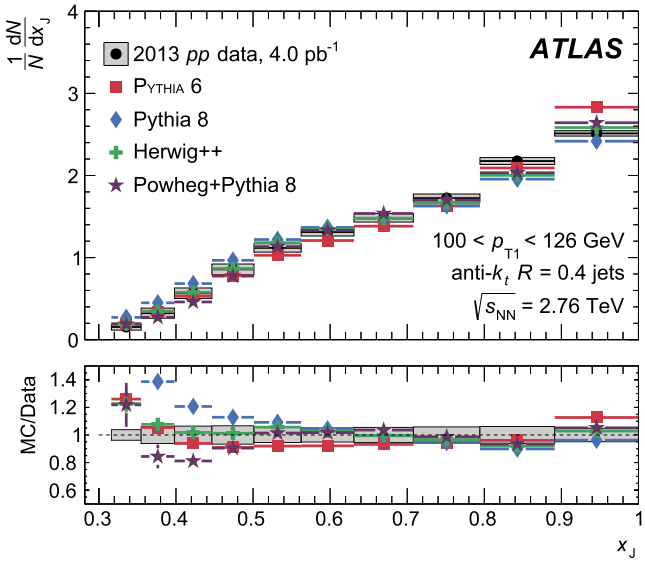


**Fig. 7.** The $(1/N)dN/dx_J$ distribution for $R = 0.4$ jets in $pp$ collisions for the $100 < p_{T_1} < 126$ GeV interval is shown in black points with the grey shaded boxes indicating the systematic uncertainties. Also shown are results obtained from various MC event generators: Pythia 6 (red squares), Pythia 8 (blue diamonds), Herwig++ (green crosses) and Powheg+Pythia 8 (purple stars). The ratio of each MC result to the data is shown in the bottom panel where the systematic uncertainties of the data are indicated by a shaded band centred at unity. (For interpretation of the references to colour in this figure, the reader is referred to the web version of this article.)

CTEQ6L1 PDF set [26] except the Powheg+Pythia 8, which used the CT10 PDF set [29]. All four models describe the data fairly well with the Herwig++ and Powheg+Pythia 8 showing the best agreement over the full $x_J$ range.

The unfolded $(1/N)dN/dx_J$ distributions in Pb+Pb collisions are shown in Fig. 8, for jet pairs with $100 < p_{T_1} < 126$ GeV for different centrality intervals. The distribution in $pp$ collisions is shown on each panel for comparison. In the 60–80% centrality bin, where the effects of quenching are expected to be the smallest, the Pb+Pb data are consistent with the $pp$ data. In more central Pb+Pb collisions, the distributions become significantly broader than that in $pp$ collisions and the peak at $x_J \sim 1$, corresponding to nearly symmetric dijet events, is reduced. At lower centrality percentiles the distribution becomes almost constant over the range $0.6 \lesssim x_J \lesssim 1$, and develops a peak at $x_J \sim 0.5$ in the 0–10% centrality interval.

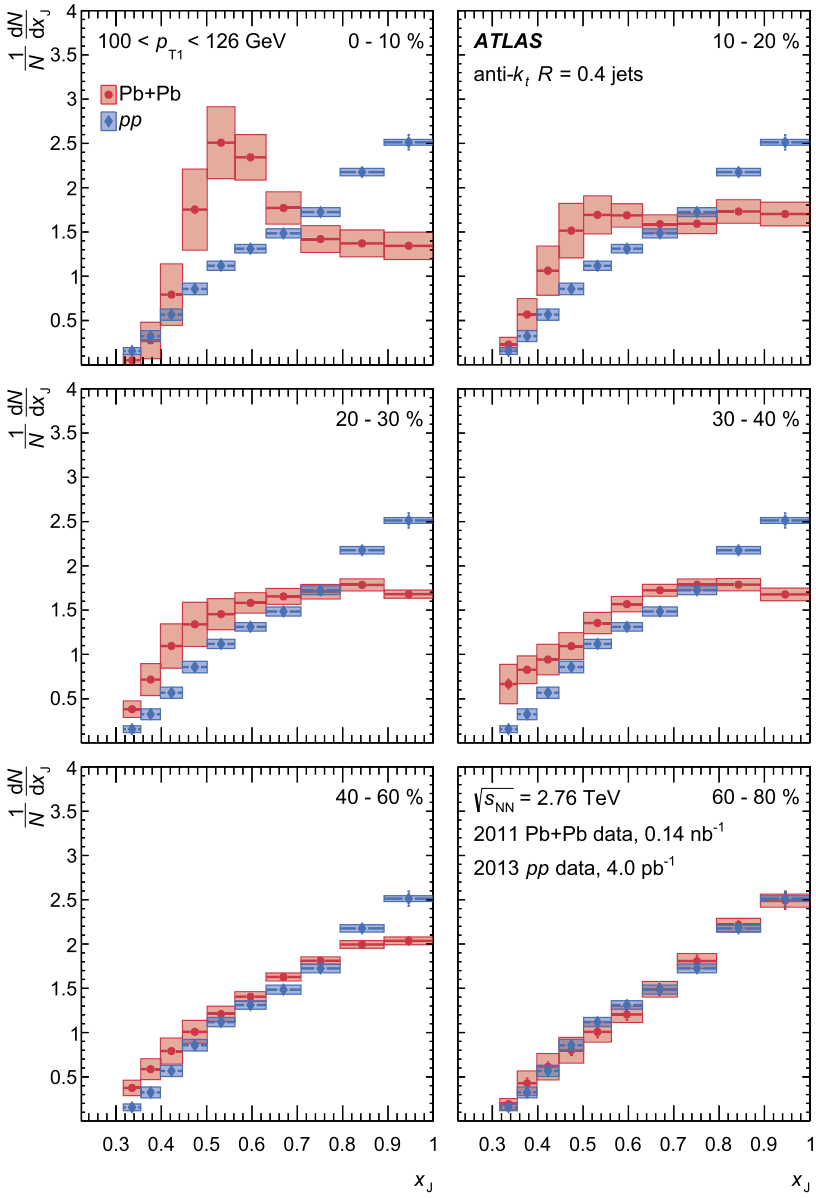


**Fig. 8.** The $(1/N)\mathrm{d}N/\mathrm{d}x_\mathrm{J}$ distributions for jet pairs with $100 < p_{\mathrm{T}_1} < 126$ GeV for different collision centralities for $R = 0.4$ jets. The Pb+Pb data are shown in red circles, while the *pp* distribution is shown for comparison in blue diamonds, and is the same in all panels. Statistical uncertainties are indicated by the error bars while systematic uncertainties are shown with shaded boxes. (For interpretation of the references to colour in this figure, the reader is referred to the web version of this article.)

Fig. 9 shows the $(1/N)\mathrm{d}N/\mathrm{d}x_\mathrm{J}$ distributions for 0–10% centrality Pb+Pb collisions and *pp* collisions for different selections on $p_{\mathrm{T}_1}$. In *pp* collisions, the $x_\mathrm{J}$ distribution becomes increasingly narrow with increasing $p_{\mathrm{T}_1}$, indicating that higher-$p_\mathrm{T}$ dijets tend to be better balanced in momentum (fractionally). At higher $p_{\mathrm{T}_1}$, the $x_\mathrm{J}$ distribution begins to fall more steeply from $x_\mathrm{J} \sim 1$, but appears to flatten at intermediate values of $x_\mathrm{J}$. The modifications observed in the Pb+Pb data lessen with increasing $p_{\mathrm{T}_1}$ and for jet pairs with $p_{\mathrm{T}_1} > 200$ GeV the maximum at $x_\mathrm{J} \sim 1$ is restored.

The distributions for $R = 0.3$ jets are also shown for the 0–10% centrality interval and for *pp* collisions for different $p_{\mathrm{T}_1}$ ranges in Fig. 10. The $p_\mathrm{T}$ of an $R = 0.3$ jet is generally lower than that of an $R = 0.4$ jet originating from the same hard scattering, and thus features observed in the $(1/N)\mathrm{d}N/\mathrm{d}x_\mathrm{J}$ distributions for $R = 0.4$ jets are expected to appear at lower values of $p_{\mathrm{T}_1}$ for $R = 0.3$ jets. To facilitate a comparison between results obtained with the two $R$ values, the $R = 0.3$ jet results include an additional $p_{\mathrm{T}_1}$ interval, $79 < p_{\mathrm{T}_1} < 100$ GeV. The differences between the Pb+Pb and *pp* $(1/N)\mathrm{d}N/\mathrm{d}x_\mathrm{J}$ distributions are qualitatively similar to those observed for $R = 0.4$ jets. Fig. 11 shows the $(1/N)\mathrm{d}N/\mathrm{d}x_\mathrm{J}$ distributions for $79 < p_{\mathrm{T}_1} < 100$ GeV for different collision centralities but for jets reconstructed with $R = 0.3$. This indicates that the trends present in $p_{\mathrm{T}_1}$ and centrality are robust with respect to the UE and that UE effects are properly accounted for by the combinatoric subtraction and unfolding procedures applied in the data analysis. The distributions are flatter for $R = 0.3$ jets in all $p_\mathrm{T}$ and centrality bins, including in *pp* collisions. This is consistent with the expectation that the $(p_{\mathrm{T}_1}, p_{\mathrm{T}_2})$ correlation is weaker for smaller-$R$ jets due to the effects of parton radiation outside the nominal jet cone.

## 9. Conclusion

This Letter presents a measurement of dijet $x_\mathrm{J}$ distributions in 4.0 pb$^{-1}$ of *pp* and 0.14 nb$^{-1}$ of Pb+Pb collisions at $\sqrt{s_{\mathrm{NN}}} = 2.76$ TeV. The measurement is performed differentially in leading-jet transverse momentum, $p_{\mathrm{T}_1}$, and in collision centrality using

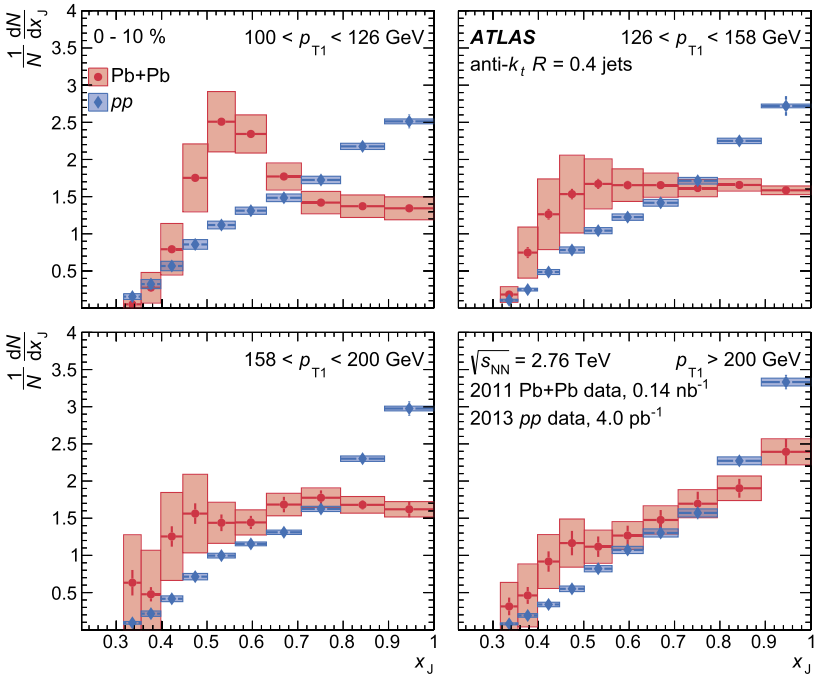


**Fig. 9.** The $(1/N)\mathrm{d}N/\mathrm{d}x_\mathrm{J}$ distributions for $R = 0.4$ jets with different selections on $p_{\mathrm{T_1}}$, shown for the 0–10% centrality bin (red circles) and for $pp$ (blue diamonds). Statistical uncertainties are indicated by the error bars while systematic uncertainties are shown with shaded boxes. (For interpretation of the references to colour in this figure, the reader is referred to the web version of this article.)

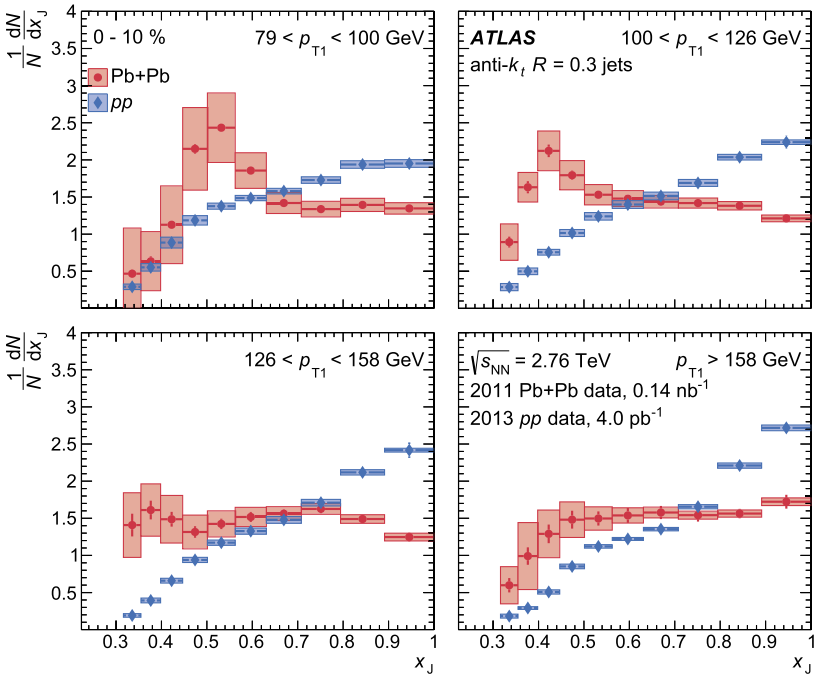


**Fig. 10.** The $(1/N)\mathrm{d}N/\mathrm{d}x_\mathrm{J}$ distributions for $R = 0.3$ jets with different selections on $p_{\mathrm{T_1}}$, shown for the 0–10% centrality bin (red circles) and for $pp$ (blue diamonds). Statistical uncertainties are indicated by the error bars while systematic uncertainties are shown with shaded boxes. (For interpretation of the references to colour in this figure, the reader is referred to the web version of this article.)

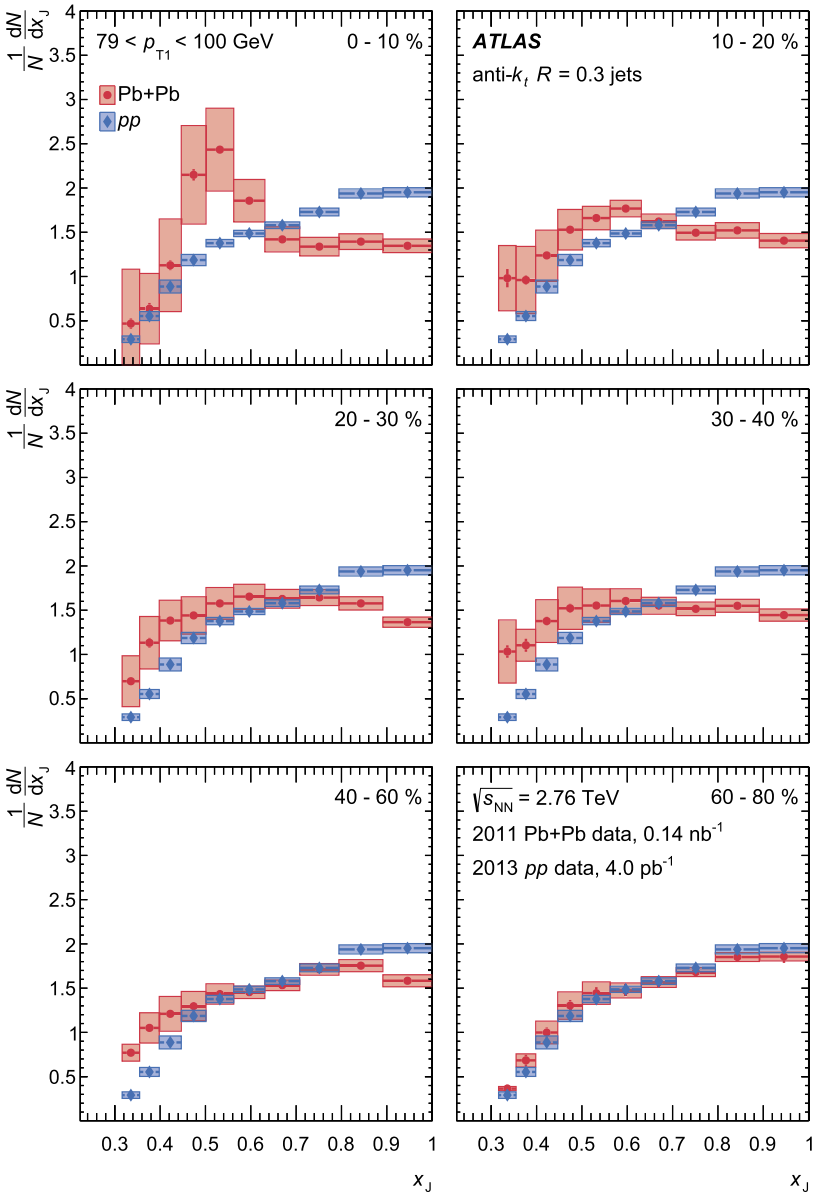


**Fig. 11.** The $(1/N)dN/dx_J$ distributions for jet pairs with $79 < p_{T_1} < 100$ GeV for different collision centralities for $R = 0.3$ jets. The Pb+Pb data are shown in red circles, while the *pp* distribution is shown for comparison in blue diamonds, and is the same in all panels. Statistical uncertainties are indicated by the error bars while systematic uncertainties are shown with shaded boxes. (For interpretation of the references to colour in this figure, the reader is referred to the web version of this article.)

data from the ATLAS detector at the LHC. The measured distributions are unfolded to account for the effects of experimental resolution and inefficiencies on the two-dimensional $(p_{T_1}, p_{T_2})$ distributions and then projected into bins of fixed ratio $x_J = p_{T_2}/p_{T_1}$. The distributions show a larger contribution of asymmetric dijets in Pb+Pb data compared to that in *pp* data, a feature that becomes more pronounced in more central collisions and is consistent with expectations of medium-induced energy loss due to jet quenching. In the 0–10% centrality bin for $100 < p_{T_1} < 126$ GeV, the $x_J$ distribution develops a significant peak at $x_J \sim 0.5$ indicating that the most probable configuration for dijets is for them to be highly unbalanced. This is in sharp contrast to the situation in the *pp* data where the most probable values are near $x_J \sim 1$. The centrality-dependent modifications evolve smoothly from central to peripheral collisions, and the results in the 60–80% centrality bin and the *pp* data are consistent. At larger values of $p_{T_1}$ the $x_J$ distributions are observed to narrow and the differences between the distributions in central Pb+Pb and *pp* collisions lessen. This is qualitatively consistent with a picture in which the fractional energy loss decreases with increasing jet $p_T$. The features in the data are compatible with those observed in previous measurements of dijets in Pb+Pb collisions by the ATLAS and CMS collaborations, however, the trends in this measurement are more prominent due to the application of the unfolding procedure. This result constitutes an important benchmark for theoretical models of jet quenching and the dynamics of relativistic heavy-ion collisions.

## Acknowledgements

We thank CERN for the very successful operation of the LHC, as well as the support staff from our institutions without whom ATLAS could not be operated efficiently.

We acknowledge the support of ANPCyT, Argentina; YerPhI, Armenia; ARC, Australia; BMWFW and FWF, Austria; ANAS, Azerbaijan; SSTC, Belarus; CNPq and FAPESP, Brazil; NSERC, NRC and CFI, Canada; CERN; CONICYT, Chile; CAS, MOST and NSFC, China;

COLCIENCIAS, Colombia; MSMT CR, MPO CR and VSC CR, Czech Republic; DNRF and DNSRC, Denmark; IN2P3-CNRS, CEA-DSM/IRFU, France; SRNSF, Georgia; BMBF, HGF, and MPG, Germany; GSRT, Greece; RGC, Hong Kong SAR, China; ISF, I-CORE and Benoziyo Center, Israel; INFN, Italy; MEXT and JSPS, Japan; CNRST, Morocco; NWO, Netherlands; RCN, Norway; MNiSW and NCN, Poland; FCT, Portugal; MNE/IFA, Romania; MES of Russia and NRC KI, Russian Federation; JINR; MESTD, Serbia; MSSR, Slovakia; ARRS and MIZŠ, Slovenia; DST/NRF, South Africa; MINECO, Spain; SRC and Wallenberg Foundation, Sweden; SERI, SNSF and Cantons of Bern and Geneva, Switzerland; MOST, Taiwan; TAEK, Turkey; STFC, United Kingdom; DOE and NSF, United States of America. In addition, individual groups and members have received support from BCKDF, the Canada Council, Canarie, CRC, Compute Canada, FQRNT, and the Ontario Innovation Trust, Canada; EPLANET, ERC, ERDF, FP7, Horizon 2020 and Marie Skłodowska-Curie Actions, European Union; Investissements d'Avenir Labex and Idex, ANR, Région Auvergne and Fondation Partager le Savoir, France; DFG and AvH Foundation, Germany; Herakleitos, Thales and Aristeia programmes co-financed by EU-ESF and the Greek NSRF; BSF, GIF and Minerva, Israel; BRF, Norway; CERCA Programme Generalitat de Catalunya, Generalitat Valenciana, Spain; the Royal Society and Leverhulme Trust, United Kingdom.

The crucial computing support from all WLCG partners is acknowledged gratefully, in particular from CERN, the ATLAS Tier-1 facilities at TRIUMF (Canada), NDGF (Denmark, Norway, Sweden), CC-IN2P3 (France), KIT/GridKA (Germany), INFN-CNAF (Italy), NL-T1 (Netherlands), PIC (Spain), ASGC (Taiwan), RAL (UK) and BNL (USA), the Tier-2 facilities worldwide and large non-WLCG resource providers. Major contributors of computing resources are listed in Ref. [43].

## References

[1] PHENIX Collaboration, K. Adcox, et al., Formation of dense partonic matter in relativistic nucleus nucleus collisions at RHIC: experimental evaluation by the PHENIX collaboration, Nucl. Phys. A 757 (2005) 184, arXiv:nucl-ex/0410003.
[2] STAR Collaboration, J. Adams, et al., Experimental and theoretical challenges in the search for the quark gluon plasma: the STAR collaboration's critical assessment of the evidence from RHIC collisions, Nucl. Phys. A 757 (2005) 102, arXiv:nucl-ex/0501009.
[3] ATLAS Collaboration, Observation of a centrality-dependent dijet asymmetry in lead–lead collisions at $\sqrt{s_{\mathrm{NN}}} = 2.76$ TeV with the ATLAS detector at the LHC, Phys. Rev. Lett. 105 (2010) 252303, arXiv:1011.6182 [hep-ex].
[4] J.D. Bjorken, Energy loss of energetic partons in quark–gluon plasma: possible extinction of high $p_T$ jets in hadron–hadron collisions, FERMILAB-PUB-82-059-THY, 1982.
[5] ATLAS Collaboration, Measurement of the jet radius and transverse momentum dependence of inclusive jet suppression in lead–lead collisions at $\sqrt{s_{\mathrm{NN}}} = 2.76$ TeV with the ATLAS detector, Phys. Lett. B 719 (2013) 220, arXiv:1208.1967 [hep-ex].
[6] ATLAS Collaboration, Measurements of the nuclear modification factor for jets in Pb+Pb collisions at $\sqrt{s_{\mathrm{NN}}} = 2.76$ TeV with the ATLAS detector, Phys. Rev. Lett. 114 (2015) 072302, arXiv:1411.2357 [hep-ex].
[7] ATLAS Collaboration, Measurement of the azimuthal angle dependence of inclusive jet yields in Pb+Pb collisions at $\sqrt{s_{\mathrm{NN}}} = 2.76$ TeV with the ATLAS detector, Phys. Rev. Lett. 111 (2013) 152301, arXiv:1306.6469 [hep-ex].
[8] CMS Collaboration, Observation and studies of jet quenching in PbPb collisions at $\sqrt{s_{\mathrm{NN}}} = 2.76$ TeV, Phys. Rev. C 84 (2011) 024906, arXiv:1102.1957 [hep-ex].
[9] CMS Collaboration, Jet momentum dependence of jet quenching in PbPb collisions at $\sqrt{s_{\mathrm{NN}}} = 2.76$ TeV, Phys. Lett. B 712 (2012) 176, arXiv:1202.5022 [hep-ex].
[10] CMS Collaboration, Studies of jet quenching using isolated-photon+jet correlations in PbPb and $pp$ collisions at $\sqrt{s_{\mathrm{NN}}} = 2.76$ TeV, Phys. Lett. B 718 (2013) 773, arXiv:1205.0206 [hep-ex].
[11] ATLAS Collaboration, Measurement of inclusive jet charged-particle fragmentation functions in Pb+Pb collisions at $\sqrt{s_{\mathrm{NN}}} = 2.76$ TeV with the ATLAS detector, Phys. Lett. B 739 (2014) 320, arXiv:1406.2979 [hep-ex].
[12] CMS Collaboration, Measurement of jet fragmentation into charged particles in $pp$ and PbPb collisions at $\sqrt{s_{\mathrm{NN}}} = 2.76$ TeV, J. High Energy Phys. 10 (2012) 087, arXiv:1205.5872 [hep-ex].
[13] CMS Collaboration, Measurement of jet fragmentation in PbPb and $pp$ collisions at $\sqrt{s_{\mathrm{NN}}} = 2.76$ TeV, Phys. Rev. C 90 (2014) 024908, arXiv:1406.0932 [hep-ex].
[14] ALICE Collaboration, B. Abelev, et al., Measurement of charged jet suppression in Pb-Pb collisions at $\sqrt{s_{NN}} = 2.76$ TeV, J. High Energy Phys. 03 (2014) 013, arXiv:1311.0633 [nucl-ex].
[15] M. Cacciari, G.P. Salam, G. Soyez, The anti-$k_t$ jet clustering algorithm, J. High Energy Phys. 04 (2008) 063, arXiv:0802.1189 [hep-ph].
[16] ATLAS Collaboration, The ATLAS experiment at the CERN Large Hadron Collider, J. Instrum. 3 (2008) S08003.
[17] ATLAS Collaboration, Measurement of the pseudorapidity and transverse momentum dependence of the elliptic flow of charged particles in lead–lead collisions at $\sqrt{s_{\mathrm{NN}}} = 2.76$ TeV with the ATLAS detector, Phys. Lett. B 707 (2012) 330, arXiv:1108.6018 [hep-ex].
[18] ATLAS Collaboration, The performance of the jet trigger for the ATLAS detector during 2011 data taking, Eur. Phys. J. C 76 (2016) 526, arXiv:1606.07759 [hep-ex].
[19] ATLAS Collaboration, Jet energy measurement with the ATLAS detector in proton–proton collisions at $\sqrt{s} = 7$ TeV, Eur. Phys. J. C 73 (2013) 2304, arXiv:1112.6426 [hep-ex].
[20] M.L. Miller, et al., Glauber modeling in high energy nuclear collisions, Annu. Rev. Nucl. Part. Sci. 57 (2007) 205, arXiv:nucl-ex/0701025.
[21] B. Alver, et al., The PHOBOS Glauber Monte Carlo, arXiv:0805.4411 [nucl-ex], 2008.
[22] S. Agostinelli, et al., GEANT4: a simulation toolkit, Nucl. Instrum. Methods Phys. Res., Sect. A, Accel. Spectrom. Detect. Assoc. Equip. 506 (2003) 250.
[23] ATLAS Collaboration, The ATLAS simulation infrastructure, Eur. Phys. J. C 70 (2010) 823, arXiv:1005.4568 [hep-ex].
[24] T. Sjöstrand, S. Mrenna, P.Z. Skands, PYTHIA 6.4 physics and manual, J. High Energy Phys. 05 (2006) 026, arXiv:hep-ph/0603175.
[25] ATLAS Collaboration, ATLAS tunes of PYTHIA 6 and Pythia 8 for MC11, ATL-PHYS-PUB-2011-009, http://cdsweb.cern.ch/record/1363300, 2011.
[26] J. Pumplin, et al., New generation of parton distributions with uncertainties from global QCD analysis, J. High Energy Phys. 07 (2002) 012, arXiv:hep-ph/0201195.
[27] T. Sjöstrand, S. Mrenna, P.Z. Skands, A brief introduction to PYTHIA 8.1, Comput. Phys. Commun. 178 (2008) 852, arXiv:0710.3820 [hep-ph].
[28] ATLAS Collaboration, Summary of ATLAS Pythia 8 tunes, ATL-PHYS-PUB-2012-003, https://cds.cern.ch/record/1474107, 2012.
[29] H.-L. Lai, et al., New parton distributions for collider physics, Phys. Rev. D 82 (2010) 074024, arXiv:1007.2241 [hep-ph].
[30] I. Lokhtin, A. Snigirev, A model of jet quenching in ultrarelativistic heavy ion collisions and high-$p(T)$ hadron spectra at RHIC, Eur. Phys. J. C 45 (2006) 211, arXiv:hep-ph/0506189.
[31] M. Cacciari, G.P. Salam, G. Soyez, FastJet user manual, Eur. Phys. J. C 72 (2012) 1896, arXiv:1111.6097 [hep-ph].
[32] ATLAS Collaboration, Jet energy measurement and its systematic uncertainty in proton–proton collisions at $\sqrt{s} = 7$ TeV with the ATLAS detector, Eur. Phys. J. C 75 (2015) 17, arXiv:1406.0076 [hep-ex].
[33] ATLAS Collaboration, Measurement of the azimuthal anisotropy for charged particle production in $\sqrt{s_{\mathrm{NN}}} = 2.76$ TeV lead–lead collisions with the ATLAS detector, Phys. Rev. C 86 (2012) 014907, arXiv:1203.3087 [hep-ex].
[34] G. D'Agostini, A multidimensional unfolding method based on Bayes' theorem, Nucl. Instrum. Methods Phys. Res., Sect. A, Accel. Spectrom. Detect. Assoc. Equip. 362 (1995) 487.
[35] T. Adye, Unfolding algorithms and tests using RooUnfold, arXiv:1105.1160 [physics.data-an], 2011.
[36] ATLAS Collaboration, Jet energy resolution in proton–proton collisions at $\sqrt{s} = 7$ TeV recorded in 2010 with the ATLAS detector, Eur. Phys. J. C 73 (2013) 2306, arXiv:1210.6210 [hep-ex].
[37] ATLAS Collaboration, Study of jet shapes in inclusive jet production in $pp$ collisions at $\sqrt{s} = 7$ TeV using the ATLAS detector, Phys. Rev. D 83 (2011) 052003, arXiv:1101.0070 [hep-ex].
[38] M. Bahr, et al., Herwig++ physics and manual, Eur. Phys. J. C 58 (2008) 639, arXiv:0803.0883 [hep-ph].
[39] S. Gieseke, C. Rohr, A. Siodmok, Colour reconnections in Herwig++, Eur. Phys. J. C 72 (2012) 2225, arXiv:1206.0041 [hep-ph].
[40] P. Nason, A new method for combining NLO QCD with shower Monte Carlo algorithms, J. High Energy Phys. 11 (2004) 040, arXiv:hep-ph/0409146.
[41] S. Frixione, P. Nason, C. Oleari, Matching NLO QCD computations with parton shower simulations: the POWHEG method, J. High Energy Phys. 11 (2007) 070, arXiv:0709.2092 [hep-ph].
[42] S. Alioli, et al., A general framework for implementing NLO calculations in shower Monte Carlo programs: the POWHEG BOX, J. High Energy Phys. 06 (2010) 043, arXiv:1002.2581 [hep-ph].
[43] ATLAS Collaboration, ATLAS computing acknowledgements 2016–2017, ATL-GEN-PUB-2016-002, 2016, https://cdsweb.cern.ch/record/2202407.

**The ATLAS Collaboration**

M. Aaboud [137d], G. Aad [88], B. Abbott [115], J. Abdallah [8], O. Abdinov [12], B. Abeloos [119], S.H. Abidi [161], O.S. AbouZeid [139], N.L. Abraham [151], H. Abramowicz [155], H. Abreu [154], R. Abreu [118], Y. Abulaiti [148a,148b], B.S. Acharya [167a,167b,a], S. Adachi [157], L. Adamczyk [41a], D.L. Adams [27], J. Adelman [110], M. Adersberger [102], T. Adye [133], A.A. Affolder [139], T. Agatonovic-Jovin [14], C. Agheorghiesei [28b], J.A. Aguilar-Saavedra [128a,128f], S.P. Ahlen [24], F. Ahmadov [68,b], G. Aielli [135a,135b], S. Akatsuka [71], H. Akerstedt [148a,148b], T.P.A. Åkesson [84], A.V. Akimov [98], G.L. Alberghi [22a,22b], J. Albert [172], M.J. Alconada Verzini [74], M. Aleksa [32], I.N. Aleksandrov [68], C. Alexa [28b], G. Alexander [155], T. Alexopoulos [10], M. Alhroob [115], B. Ali [130], M. Aliev [76a,76b], G. Alimonti [94a], J. Alison [33], S.P. Alkire [38], B.M.M. Allbrooke [151], B.W. Allen [118], P.P. Allport [19], A. Aloisio [106a,106b], A. Alonso [39], F. Alonso [74], C. Alpigiani [140], A.A. Alshehri [56], M. Alstaty [88], B. Alvarez Gonzalez [32], D. Álvarez Piqueras [170], M.G. Alviggi [106a,106b], B.T. Amadio [16], Y. Amaral Coutinho [26a], C. Amelung [25], D. Amidei [92], S.P. Amor Dos Santos [128a,128c], A. Amorim [128a,128b], S. Amoroso [32], G. Amundsen [25], C. Anastopoulos [141], L.S. Ancu [52], N. Andari [19], T. Andeen [11], C.F. Anders [60b], J.K. Anders [77], K.J. Anderson [33], A. Andreazza [94a,94b], V. Andrei [60a], S. Angelidakis [9], I. Angelozzi [109], A. Angerami [38], F. Anghinolfi [32], A.V. Anisenkov [111,c], N. Anjos [13], A. Annovi [126a,126b], C. Antel [60a], M. Antonelli [50], A. Antonov [100,*], D.J. Antrim [166], F. Anulli [134a], M. Aoki [69], L. Aperio Bella [32], G. Arabidze [93], Y. Arai [69], J.P. Araque [128a], V. Araujo Ferraz [26a], A.T.H. Arce [48], R.E. Ardell [80], F.A. Arduh [74], J-F. Arguin [97], S. Argyropoulos [66], M. Arik [20a], A.J. Armbruster [145], L.J. Armitage [79], O. Arnaez [32], H. Arnold [51], M. Arratia [30], O. Arslan [23], A. Artamonov [99], G. Artoni [122], S. Artz [86], S. Asai [157], N. Asbah [45], A. Ashkenazi [155], L. Asquith [151], K. Assamagan [27], R. Astalos [146a], M. Atkinson [169], N.B. Atlay [143], K. Augsten [130], G. Avolio [32], B. Axen [16], M.K. Ayoub [119], G. Azuelos [97,d], A.E. Baas [60a], M.J. Baca [19], H. Bachacou [138], K. Bachas [76a,76b], M. Backes [122], M. Backhaus [32], P. Bagiacchi [134a,134b], P. Bagnaia [134a,134b], J.T. Baines [133], M. Bajic [39], O.K. Baker [179], E.M. Baldin [111,c], P. Balek [175], T. Balestri [150], F. Balli [138], W.K. Balunas [124], E. Banas [42], Sw. Banerjee [176,e], A.A.E. Bannoura [178], L. Barak [32], E.L. Barberio [91], D. Barberis [53a,53b], M. Barbero [88], T. Barillari [103], M-S Barisits [32], T. Barklow [145], N. Barlow [30], S.L. Barnes [36c], B.M. Barnett [133], R.M. Barnett [16], Z. Barnovska-Blenessy [36a], A. Baroncelli [136a], G. Barone [25], A.J. Barr [122], L. Barranco Navarro [170], F. Barreiro [85], J. Barreiro Guimarães da Costa [35a], R. Bartoldus [145], A.E. Barton [75], P. Bartos [146a], A. Basalaev [125], A. Bassalat [119,f], R.L. Bates [56], S.J. Batista [161], J.R. Batley [30], M. Battaglia [139], M. Bauce [134a,134b], F. Bauer [138], H.S. Bawa [145,g], J.B. Beacham [113], M.D. Beattie [75], T. Beau [83], P.H. Beauchemin [165], P. Bechtle [23], H.P. Beck [18,h], K. Becker [122], M. Becker [86], M. Beckingham [173], C. Becot [112], A.J. Beddall [20d], A. Beddall [20b], V.A. Bednyakov [68], M. Bedognetti [109], C.P. Bee [150], T.A. Beermann [32], M. Begalli [26a], M. Begel [27], J.K. Behr [45], A.S. Bell [81], G. Bella [155], L. Bellagamba [22a], A. Bellerive [31], M. Bellomo [89], K. Belotskiy [100], O. Beltramello [32], N.L. Belyaev [100], O. Benary [155,*], D. Benchekroun [137a], M. Bender [102], K. Bendtz [148a,148b], N. Benekos [10], Y. Benhammou [155], E. Benhar Noccioli [179], J. Benitez [66], D.P. Benjamin [48], M. Benoit [52], J.R. Bensinger [25], S. Bentvelsen [109], L. Beresford [122], M. Beretta [50], D. Berge [109], E. Bergeaas Kuutmann [168], N. Berger [5], J. Beringer [16], S. Berlendis [58], N.R. Bernard [89], G. Bernardi [83], C. Bernius [112], F.U. Bernlochner [23], T. Berry [80], P. Berta [131], C. Bertella [86], G. Bertoli [148a,148b], F. Bertolucci [126a,126b], I.A. Bertram [75], C. Bertsche [45], D. Bertsche [115], G.J. Besjes [39], O. Bessidskaia Bylund [148a,148b], M. Bessner [45], N. Besson [138], C. Betancourt [51], A. Bethani [87], S. Bethke [103], A.J. Bevan [79], R.M. Bianchi [127], M. Bianco [32], O. Biebel [102], D. Biedermann [17], R. Bielski [87], N.V. Biesuz [126a,126b], M. Biglietti [136a], J. Bilbao De Mendizabal [52], T.R.V. Billoud [97], H. Bilokon [50], M. Bindi [57], A. Bingul [20b], C. Bini [134a,134b], S. Biondi [22a,22b], T. Bisanz [57], C. Bittrich [47], D.M. Bjergaard [48], C.W. Black [152], J.E. Black [145], K.M. Black [24], D. Blackburn [140], R.E. Blair [6], T. Blazek [146a], I. Bloch [45], C. Blocker [25], A. Blue [56], W. Blum [86,*], U. Blumenschein [79], S. Blunier [34a], G.J. Bobbink [109], V.S. Bobrovnikov [111,c], S.S. Bocchetta [84], A. Bocci [48], C. Bock [102], M. Boehler [51], D. Boerner [178], D. Bogavac [102], A.G. Bogdanchikov [111], C. Bohm [148a], V. Boisvert [80], P. Bokan [168,i], T. Bold [41a], A.S. Boldyrev [101], M. Bomben [83], M. Bona [79], M. Boonekamp [138], A. Borisov [132], G. Borissov [75], J. Bortfeldt [32], D. Bortoletto [122], V. Bortolotto [62a,62b,62c], D. Boscherini [22a], M. Bosman [13], J.D. Bossio Sola [29], J. Boudreau [127], J. Bouffard [2], E.V. Bouhova-Thacker [75], D. Boumediene [37], C. Bourdarios [119], S.K. Boutle [56], A. Boveia [113], J. Boyd [32], I.R. Boyko [68], J. Bracinik [19], A. Brandt [8], G. Brandt [57], O. Brandt [60a], U. Bratzler [158], B. Brau [89], J.E. Brau [118], W.D. Breaden Madden [56], K. Brendlinger [45], A.J. Brennan [91], L. Brenner [109], R. Brenner [168], S. Bressler [175], D.L. Briglin [19],

T.M. Bristow [49], D. Britton [56], D. Britzger [45], F.M. Brochu [30], I. Brock [23], R. Brock [93], G. Brooijmans [38], T. Brooks [80], W.K. Brooks [34b], J. Brosamer [16], E. Brost [110], J.H. Broughton [19], P.A. Bruckman de Renstrom [42], D. Bruncko [146b], A. Bruni [22a], G. Bruni [22a], L.S. Bruni [109], B.H. Brunt [30], M. Bruschi [22a], N. Bruscino [23], P. Bryant [33], L. Bryngemark [84], T. Buanes [15], Q. Buat [144], P. Buchholz [143], A.G. Buckley [56], I.A. Budagov [68], F. Buehrer [51], M.K. Bugge [121], O. Bulekov [100], D. Bullock [8], H. Burckhart [32], S. Burdin [77], C.D. Burgard [51], A.M. Burger [5], B. Burghgrave [110], K. Burka [42], S. Burke [133], I. Burmeister [46], J.T.P. Burr [122], E. Busato [37], D. Büscher [51], V. Büscher [86], P. Bussey [56], J.M. Butler [24], C.M. Buttar [56], J.M. Butterworth [81], P. Butti [32], W. Buttinger [27], A. Buzatu [35c], A.R. Buzykaev [111,c], S. Cabrera Urbán [170], D. Caforio [130], V.M. Cairo [40a,40b], O. Cakir [4a], N. Calace [52], P. Calafiura [16], A. Calandri [88], G. Calderini [83], P. Calfayan [64], G. Callea [40a,40b], L.P. Caloba [26a], S. Calvente Lopez [85], D. Calvet [37], S. Calvet [37], T.P. Calvet [88], R. Camacho Toro [33], S. Camarda [32], P. Camarri [135a,135b], D. Cameron [121], R. Caminal Armadans [169], C. Camincher [58], S. Campana [32], M. Campanelli [81], A. Camplani [94a,94b], A. Campoverde [143], V. Canale [106a,106b], M. Cano Bret [36c], J. Cantero [116], T. Cao [155], M.D.M. Capeans Garrido [32], I. Caprini [28b], M. Caprini [28b], M. Capua [40a,40b], R.M. Carbone [38], R. Cardarelli [135a], F. Cardillo [51], I. Carli [131], T. Carli [32], G. Carlino [106a], B.T. Carlson [127], L. Carminati [94a,94b], R.M.D. Carney [148a,148b], S. Caron [108], E. Carquin [34b], G.D. Carrillo-Montoya [32], J. Carvalho [128a,128c], D. Casadei [19], M.P. Casado [13,j], M. Casolino [13], D.W. Casper [166], R. Castelijn [109], A. Castelli [109], V. Castillo Gimenez [170], N.F. Castro [128a,k], A. Catinaccio [32], J.R. Catmore [121], A. Cattai [32], J. Caudron [23], V. Cavaliere [169], E. Cavallaro [13], D. Cavalli [94a], M. Cavalli-Sforza [13], V. Cavasinni [126a,126b], E. Celebi [20a], F. Ceradini [136a,136b], L. Cerda Alberich [170], A.S. Cerqueira [26b], A. Cerri [151], L. Cerrito [135a,135b], F. Cerutti [16], A. Cervelli [18], S.A. Cetin [20c], A. Chafaq [137a], D. Chakraborty [110], S.K. Chan [59], W.S. Chan [109], Y.L. Chan [62a], P. Chang [169], J.D. Chapman [30], D.G. Charlton [19], A. Chatterjee [52], C.C. Chau [161], C.A. Chavez Barajas [151], S. Che [113], S. Cheatham [167a,167c], A. Chegwidden [93], S. Chekanov [6], S.V. Chekulaev [163a], G.A. Chelkov [68,l], M.A. Chelstowska [32], C. Chen [67], H. Chen [27], S. Chen [35b], S. Chen [157], X. Chen [35c,m], Y. Chen [70], H.C. Cheng [92], H.J. Cheng [35a], Y. Cheng [33], A. Cheplakov [68], E. Cheremushkina [132], R. Cherkaoui El Moursli [137e], V. Chernyatin [27,*], E. Cheu [7], L. Chevalier [138], V. Chiarella [50], G. Chiarelli [126a,126b], G. Chiodini [76a], A.S. Chisholm [32], A. Chitan [28b], Y.H. Chiu [172], M.V. Chizhov [68], K. Choi [64], A.R. Chomont [37], S. Chouridou [9], B.K.B. Chow [102], V. Christodoulou [81], D. Chromek-Burckhart [32], M.C. Chu [62a], J. Chudoba [129], A.J. Chuinard [90], J.J. Chwastowski [42], L. Chytka [117], A.K. Ciftci [4a], D. Cinca [46], V. Cindro [78], I.A. Cioara [23], C. Ciocca [22a,22b], A. Ciocio [16], F. Cirotto [106a,106b], Z.H. Citron [175], M. Citterio [94a], M. Ciubancan [28b], A. Clark [52], B.L. Clark [59], M.R. Clark [38], P.J. Clark [49], R.N. Clarke [16], C. Clement [148a,148b], Y. Coadou [88], M. Cobal [167a,167c], A. Coccaro [52], J. Cochran [67], L. Colasurdo [108], B. Cole [38], A.P. Colijn [109], J. Collot [58], T. Colombo [166], P. Conde Muiño [128a,128b], E. Coniavitis [51], S.H. Connell [147b], I.A. Connelly [87], V. Consorti [51], S. Constantinescu [28b], G. Conti [32], F. Conventi [106a,n], M. Cooke [16], B.D. Cooper [81], A.M. Cooper-Sarkar [122], F. Cormier [171], K.J.R. Cormier [161], T. Cornelissen [178], M. Corradi [134a,134b], F. Corriveau [90,o], A. Cortes-Gonzalez [32], G. Cortiana [103], G. Costa [94a], M.J. Costa [170], D. Costanzo [141], G. Cottin [30], G. Cowan [80], B.E. Cox [87], K. Cranmer [112], S.J. Crawley [56], R.A. Creager [124], G. Cree [31], S. Crépé-Renaudin [58], F. Crescioli [83], W.A. Cribbs [148a,148b], M. Crispin Ortuzar [122], M. Cristinziani [23], V. Croft [108], G. Crosetti [40a,40b], A. Cueto [85], T. Cuhadar Donszelmann [141], J. Cummings [179], M. Curatolo [50], J. Cúth [86], H. Czirr [143], P. Czodrowski [32], G. D'amen [22a,22b], S. D'Auria [56], M. D'Onofrio [77], M.J. Da Cunha Sargedas De Sousa [128a,128b], C. Da Via [87], W. Dabrowski [41a], T. Dado [146a], T. Dai [92], O. Dale [15], F. Dallaire [97], C. Dallapiccola [89], M. Dam [39], J.R. Dandoy [124], N.P. Dang [51], A.C. Daniells [19], N.S. Dann [87], M. Danninger [171], M. Dano Hoffmann [138], V. Dao [150], G. Darbo [53a], S. Darmora [8], J. Dassoulas [3], A. Dattagupta [118], T. Daubney [45], W. Davey [23], C. David [45], T. Davidek [131], M. Davies [155], P. Davison [81], E. Dawe [91], I. Dawson [141], K. De [8], R. de Asmundis [106a], A. De Benedetti [115], S. De Castro [22a,22b], S. De Cecco [83], N. De Groot [108], P. de Jong [109], H. De la Torre [93], F. De Lorenzi [67], A. De Maria [57], D. De Pedis [134a], A. De Salvo [134a], U. De Sanctis [151], A. De Santo [151], K. De Vasconcelos Corga [88], J.B. De Vivie De Regie [119], W.J. Dearnaley [75], R. Debbe [27], C. Debenedetti [139], D.V. Dedovich [68], N. Dehghanian [3], I. Deigaard [109], M. Del Gaudio [40a,40b], J. Del Peso [85], T. Del Prete [126a,126b], D. Delgove [119], F. Deliot [138], C.M. Delitzsch [52], A. Dell'Acqua [32], L. Dell'Asta [24], M. Dell'Orso [126a,126b], M. Della Pietra [106a,106b], D. della Volpe [52], M. Delmastro [5], P.A. Delsart [58], D.A. DeMarco [161], S. Demers [179], M. Demichev [68], A. Demilly [83], S.P. Denisov [132], D. Denysiuk [138],

D. Derendarz [42], J.E. Derkaoui [137d], F. Derue [83], P. Dervan [77], K. Desch [23], C. Deterre [45], K. Dette [46], P.O. Deviveiros [32], A. Dewhurst [133], S. Dhaliwal [25], A. Di Ciaccio [135a,135b], L. Di Ciaccio [5], W.K. Di Clemente [124], C. Di Donato [106a,106b], A. Di Girolamo [32], B. Di Girolamo [32], B. Di Micco [136a,136b], R. Di Nardo [32], K.F. Di Petrillo [59], A. Di Simone [51], R. Di Sipio [161], D. Di Valentino [31], C. Diaconu [88], M. Diamond [161], F.A. Dias [49], M.A. Diaz [34a], E.B. Diehl [92], J. Dietrich [17], S. Díez Cornell [45], A. Dimitrievska [14], J. Dingfelder [23], P. Dita [28b], S. Dita [28b], F. Dittus [32], F. Djama [88], T. Djobava [54b], J.I. Djuvsland [60a], M.A.B. do Vale [26c], D. Dobos [32], M. Dobre [28b], C. Doglioni [84], J. Dolejsi [131], Z. Dolezal [131], M. Donadelli [26d], S. Donati [126a,126b], P. Dondero [123a,123b], J. Donini [37], J. Dopke [133], A. Doria [106a], M.T. Dova [74], A.T. Doyle [56], E. Drechsler [57], M. Dris [10], Y. Du [36b], J. Duarte-Campderros [155], E. Duchovni [175], G. Duckeck [102], O.A. Ducu [97,p], D. Duda [109], A. Dudarev [32], A. Chr. Dudder [86], E.M. Duffield [16], L. Duflot [119], M. Dührssen [32], M. Dumancic [175], A.E. Dumitriu [28b], A.K. Duncan [56], M. Dunford [60a], H. Duran Yildiz [4a], M. Düren [55], A. Durglishvili [54b], D. Duschinger [47], B. Dutta [45], M. Dyndal [45], C. Eckardt [45], K.M. Ecker [103], R.C. Edgar [92], T. Eifert [32], G. Eigen [15], K. Einsweiler [16], T. Ekelof [168], M. El Kacimi [137c], V. Ellajosyula [88], M. Ellert [168], S. Elles [5], F. Ellinghaus [178], A.A. Elliot [172], N. Ellis [32], J. Elmsheuser [27], M. Elsing [32], D. Emeliyanov [133], Y. Enari [157], O.C. Endner [86], J.S. Ennis [173], J. Erdmann [46], A. Ereditato [18], G. Ernis [178], M. Ernst [27], S. Errede [169], E. Ertel [86], M. Escalier [119], H. Esch [46], C. Escobar [127], B. Esposito [50], A.I. Etienvre [138], E. Etzion [155], H. Evans [64], A. Ezhilov [125], F. Fabbri [22a,22b], L. Fabbri [22a,22b], G. Facini [33], R.M. Fakhrutdinov [132], S. Falciano [134a], R.J. Falla [81], J. Faltova [32], Y. Fang [35a], M. Fanti [94a,94b], A. Farbin [8], A. Farilla [136a], C. Farina [127], E.M. Farina [123a,123b], T. Farooque [93], S. Farrell [16], S.M. Farrington [173], P. Farthouat [32], F. Fassi [137e], P. Fassnacht [32], D. Fassouliotis [9], M. Faucci Giannelli [80], A. Favareto [53a,53b], W.J. Fawcett [122], L. Fayard [119], O.L. Fedin [125,q], W. Fedorko [171], S. Feigl [121], L. Feligioni [88], C. Feng [36b], E.J. Feng [32], H. Feng [92], A.B. Fenyuk [132], L. Feremenga [8], P. Fernandez Martinez [170], S. Fernandez Perez [13], J. Ferrando [45], A. Ferrari [168], P. Ferrari [109], R. Ferrari [123a], D.E. Ferreira de Lima [60b], A. Ferrer [170], D. Ferrere [52], C. Ferretti [92], F. Fiedler [86], A. Filipčič [78], M. Filipuzzi [45], F. Filthaut [108], M. Fincke-Keeler [172], K.D. Finelli [152], M.C.N. Fiolhais [128a,128c,r], L. Fiorini [170], A. Fischer [2], C. Fischer [13], J. Fischer [178], W.C. Fisher [93], N. Flaschel [45], I. Fleck [143], P. Fleischmann [92], R.R.M. Fletcher [124], T. Flick [178], B.M. Flierl [102], L.R. Flores Castillo [62a], M.J. Flowerdew [103], G.T. Forcolin [87], A. Formica [138], A. Forti [87], A.G. Foster [19], D. Fournier [119], H. Fox [75], S. Fracchia [13], P. Francavilla [83], M. Franchini [22a,22b], D. Francis [32], L. Franconi [121], M. Franklin [59], M. Frate [166], M. Fraternali [123a,123b], D. Freeborn [81], S.M. Fressard-Batraneanu [32], B. Freund [97], D. Froidevaux [32], J.A. Frost [122], C. Fukunaga [158], E. Fullana Torregrosa [86], T. Fusayasu [104], J. Fuster [170], C. Gabaldon [58], O. Gabizon [154], A. Gabrielli [22a,22b], A. Gabrielli [16], G.P. Gach [41a], S. Gadatsch [32], S. Gadomski [80], G. Gagliardi [53a,53b], L.G. Gagnon [97], P. Gagnon [64], C. Galea [108], B. Galhardo [128a,128c], E.J. Gallas [122], B.J. Gallop [133], P. Gallus [130], G. Galster [39], K.K. Gan [113], S. Ganguly [37], J. Gao [36a], Y. Gao [77], Y.S. Gao [145,g], F.M. Garay Walls [49], C. García [170], J.E. García Navarro [170], M. Garcia-Sciveres [16], R.W. Gardner [33], N. Garelli [145], V. Garonne [121], A. Gascon Bravo [45], K. Gasnikova [45], C. Gatti [50], A. Gaudiello [53a,53b], G. Gaudio [123a], I.L. Gavrilenko [98], C. Gay [171], G. Gaycken [23], E.N. Gazis [10], C.N.P. Gee [133], M. Geisen [86], M.P. Geisler [60a], K. Gellerstedt [148a,148b], C. Gemme [53a], M.H. Genest [58], C. Geng [36a,s], S. Gentile [134a,134b], C. Gentsos [156], S. George [80], D. Gerbaudo [13], A. Gershon [155], S. Ghasemi [143], M. Ghneimat [23], B. Giacobbe [22a], S. Giagu [134a,134b], P. Giannetti [126a,126b], S.M. Gibson [80], M. Gignac [171], M. Gilchriese [16], D. Gillberg [31], G. Gilles [178], D.M. Gingrich [3,d], N. Giokaris [9,*], M.P. Giordani [167a,167c], F.M. Giorgi [22a], P.F. Giraud [138], P. Giromini [59], D. Giugni [94a], F. Giuli [122], C. Giuliani [103], M. Giulini [60b], B.K. Gjelsten [121], S. Gkaitatzis [156], I. Gkialas [9,t], E.L. Gkougkousis [139], L.K. Gladilin [101], C. Glasman [85], J. Glatzer [13], P.C.F. Glaysher [45], A. Glazov [45], M. Goblirsch-Kolb [25], J. Godlewski [42], S. Goldfarb [91], T. Golling [52], D. Golubkov [132], A. Gomes [128a,128b,128d], R. Gonçalo [128a], R. Goncalves Gama [26a], J. Goncalves Pinto Firmino Da Costa [138], G. Gonella [51], L. Gonella [19], A. Gongadze [68], S. González de la Hoz [170], S. Gonzalez-Sevilla [52], L. Goossens [32], P.A. Gorbounov [99], H.A. Gordon [27], I. Gorelov [107], B. Gorini [32], E. Gorini [76a,76b], A. Gorišek [78], A.T. Goshaw [48], C. Gössling [46], M.I. Gostkin [68], C.R. Goudet [119], D. Goujdami [137c], A.G. Goussiou [140], N. Govender [147b,u], E. Gozani [154], L. Graber [57], I. Grabowska-Bold [41a], P.O.J. Gradin [58], J. Gramling [52], E. Gramstad [121], S. Grancagnolo [17], V. Gratchev [125], P.M. Gravila [28f], H.M. Gray [32], Z.D. Greenwood [82,v], C. Grefe [23], K. Gregersen [81], I.M. Gregor [45], P. Grenier [145], K. Grevtsov [5], J. Griffiths [8], A.A. Grillo [139], K. Grimm [75], S. Grinstein [13,w], Ph. Gris [37], J.-F. Grivaz [119], S. Groh [86], E. Gross [175], J. Grosse-Knetter [57], G.C. Grossi [82], Z.J. Grout [81],

L. Guan [92], W. Guan [176], J. Guenther [65], F. Guescini [163a], D. Guest [166], O. Gueta [155], B. Gui [113], E. Guido [53a,53b], T. Guillemin [5], S. Guindon [2], U. Gul [56], C. Gumpert [32], J. Guo [36c], W. Guo [92], Y. Guo [36a], R. Gupta [43], S. Gupta [122], G. Gustavino [134a,134b], P. Gutierrez [115], N.G. Gutierrez Ortiz [81], C. Gutschow [81], C. Guyot [138], M.P. Guzik [41a], C. Gwenlan [122], C.B. Gwilliam [77], A. Haas [112], C. Haber [16], H.K. Hadavand [8], A. Hadef [88], S. Hageböck [23], M. Hagihara [164], H. Hakobyan [180,*], M. Haleem [45], J. Haley [116], G. Halladjian [93], G.D. Hallewell [88], K. Hamacher [178], P. Hamal [117], K. Hamano [172], A. Hamilton [147a], G.N. Hamity [141], P.G. Hamnett [45], L. Han [36a], S. Han [35a], K. Hanagaki [69,x], K. Hanawa [157], M. Hance [139], B. Haney [124], P. Hanke [60a], R. Hanna [138], J.B. Hansen [39], J.D. Hansen [39], M.C. Hansen [23], P.H. Hansen [39], K. Hara [164], A.S. Hard [176], T. Harenberg [178], F. Hariri [119], S. Harkusha [95], R.D. Harrington [49], P.F. Harrison [173], N.M. Hartmann [102], M. Hasegawa [70], Y. Hasegawa [142], A. Hasib [49], S. Hassani [138], S. Haug [18], R. Hauser [93], L. Hauswald [47], L.B. Havener [38], M. Havranek [130], C.M. Hawkes [19], R.J. Hawkings [32], D. Hayakawa [159], D. Hayden [93], C.P. Hays [122], J.M. Hays [79], H.S. Hayward [77], S.J. Haywood [133], S.J. Head [19], T. Heck [86], V. Hedberg [84], L. Heelan [8], K.K. Heidegger [51], S. Heim [45], T. Heim [16], B. Heinemann [45,y], J.J. Heinrich [102], L. Heinrich [112], C. Heinz [55], J. Hejbal [129], L. Helary [32], A. Held [171], S. Hellman [148a,148b], C. Helsens [32], J. Henderson [122], R.C.W. Henderson [75], Y. Heng [176], S. Henkelmann [171], A.M. Henriques Correia [32], S. Henrot-Versille [119], G.H. Herbert [17], H. Herde [25], V. Herget [177], Y. Hernández Jiménez [147c], G. Herten [51], R. Hertenberger [102], L. Hervas [32], T.C. Herwig [124], G.G. Hesketh [81], N.P. Hessey [163a], J.W. Hetherly [43], S. Higashino [69], E. Higón-Rodriguez [170], E. Hill [172], J.C. Hill [30], K.H. Hiller [45], S.J. Hillier [19], I. Hinchliffe [16], M. Hirose [51], D. Hirschbuehl [178], B. Hiti [78], O. Hladik [129], X. Hoad [49], J. Hobbs [150], N. Hod [163a], M.C. Hodgkinson [141], P. Hodgson [141], A. Hoecker [32], M.R. Hoeferkamp [107], F. Hoenig [102], D. Hohn [23], T.R. Holmes [16], M. Homann [46], S. Honda [164], T. Honda [69], T.M. Hong [127], B.H. Hooberman [169], W.H. Hopkins [118], Y. Horii [105], A.J. Horton [144], J-Y. Hostachy [58], S. Hou [153], A. Hoummada [137a], J. Howarth [45], J. Hoya [74], M. Hrabovsky [117], I. Hristova [17], J. Hrivnac [119], T. Hryn'ova [5], A. Hrynevich [96], P.J. Hsu [63], S.-C. Hsu [140], Q. Hu [36a], S. Hu [36c], Y. Huang [35a], Z. Hubacek [130], F. Hubaut [88], F. Huegging [23], T.B. Huffman [122], E.W. Hughes [38], G. Hughes [75], M. Huhtinen [32], P. Huo [150], N. Huseynov [68,b], J. Huston [93], J. Huth [59], G. Iacobucci [52], G. Iakovidis [27], I. Ibragimov [143], L. Iconomidou-Fayard [119], P. Iengo [32], O. Igonkina [109,z], T. Iizawa [174], Y. Ikegami [69], M. Ikeno [69], Y. Ilchenko [11,aa], D. Iliadis [156], N. Ilic [145], G. Introzzi [123a,123b], P. Ioannou [9,*], M. Iodice [136a], K. Iordanidou [38], V. Ippolito [59], N. Ishijima [120], M. Ishino [157], M. Ishitsuka [159], C. Issever [122], S. Istin [20a], F. Ito [164], J.M. Iturbe Ponce [87], R. Iuppa [162a,162b], H. Iwasaki [69], J.M. Izen [44], V. Izzo [106a], S. Jabbar [3], P. Jackson [1], V. Jain [2], K.B. Jakobi [86], K. Jakobs [51], S. Jakobsen [32], T. Jakoubek [129], D.O. Jamin [116], D.K. Jana [82], R. Jansky [65], J. Janssen [23], M. Janus [57], P.A. Janus [41a], G. Jarlskog [84], N. Javadov [68,b], T. Javůrek [51], M. Javurkova [51], F. Jeanneau [138], L. Jeanty [16], J. Jejelava [54a,ab], A. Jelinskas [173], P. Jenni [51,ac], C. Jeske [173], S. Jézéquel [5], H. Ji [176], J. Jia [150], H. Jiang [67], Y. Jiang [36a], Z. Jiang [145], S. Jiggins [81], J. Jimenez Pena [170], S. Jin [35a], A. Jinaru [28b], O. Jinnouchi [159], H. Jivan [147c], P. Johansson [141], K.A. Johns [7], C.A. Johnson [64], W.J. Johnson [140], K. Jon-And [148a,148b], R.W.L. Jones [75], S. Jones [7], T.J. Jones [77], J. Jongmanns [60a], P.M. Jorge [128a,128b], J. Jovicevic [163a], X. Ju [176], A. Juste Rozas [13,w], M.K. Köhler [175], A. Kaczmarska [42], M. Kado [119], H. Kagan [113], M. Kagan [145], S.J. Kahn [88], T. Kaji [174], E. Kajomovitz [48], C.W. Kalderon [84], A. Kaluza [86], S. Kama [43], A. Kamenshchikov [132], N. Kanaya [157], S. Kaneti [30], L. Kanjir [78], V.A. Kantserov [100], J. Kanzaki [69], B. Kaplan [112], L.S. Kaplan [176], D. Kar [147c], K. Karakostas [10], N. Karastathis [10], M.J. Kareem [57], E. Karentzos [10], S.N. Karpov [68], Z.M. Karpova [68], K. Karthik [112], V. Kartvelishvili [75], A.N. Karyukhin [132], K. Kasahara [164], L. Kashif [176], R.D. Kass [113], A. Kastanas [149], Y. Kataoka [157], C. Kato [157], A. Katre [52], J. Katzy [45], K. Kawade [105], K. Kawagoe [73], T. Kawamoto [157], G. Kawamura [57], E.F. Kay [77], V.F. Kazanin [111,c], R. Keeler [172], R. Kehoe [43], J.S. Keller [45], J.J. Kempster [80], H. Keoshkerian [161], O. Kepka [129], B.P. Kerševan [78], S. Kersten [178], R.A. Keyes [90], M. Khader [169], F. Khalil-zada [12], A. Khanov [116], A.G. Kharlamov [111,c], T. Kharlamova [111,c], A. Khodinov [160], T.J. Khoo [52], V. Khovanskiy [99,*], E. Khramov [68], J. Khubua [54b,ad], S. Kido [70], C.R. Kilby [80], H.Y. Kim [8], S.H. Kim [164], Y.K. Kim [33], N. Kimura [156], O.M. Kind [17], B.T. King [77], D. Kirchmeier [47], J. Kirk [133], A.E. Kiryunin [103], T. Kishimoto [157], D. Kisielewska [41a], K. Kiuchi [164], O. Kivernyk [138], E. Kladiva [146b], T. Klapdor-Kleingrothaus [51], M.H. Klein [38], M. Klein [77], U. Klein [77], K. Kleinknecht [86], P. Klimek [110], A. Klimentov [27], R. Klingenberg [46], T. Klioutchnikova [32], E.-E. Kluge [60a], P. Kluit [109], S. Kluth [103], J. Knapik [42], E. Kneringer [65], E.B.F.G. Knoops [88], A. Knue [103], A. Kobayashi [157], D. Kobayashi [159], T. Kobayashi [157], M. Kobel [47], M. Kocian [145], P. Kodys [131], T. Koffas [31], E. Koffeman [109], N.M. Köhler [103],

T. Koi [145], M. Kolb [60b], I. Koletsou [5], A.A. Komar [98,*], Y. Komori [157], T. Kondo [69], N. Kondrashova [36c], K. Köneke [51], A.C. König [108], T. Kono [69,ae], R. Konoplich [112,af], N. Konstantinidis [81], R. Kopeliansky [64], S. Koperny [41a], A.K. Kopp [51], K. Korcyl [42], K. Kordas [156], A. Korn [81], A.A. Korol [111,c], I. Korolkov [13], E.V. Korolkova [141], O. Kortner [103], S. Kortner [103], T. Kosek [131], V.V. Kostyukhin [23], A. Kotwal [48], A. Koulouris [10], A. Kourkoumeli-Charalampidi [123a,123b], C. Kourkoumelis [9], V. Kouskoura [27], A.B. Kowalewska [42], R. Kowalewski [172], T.Z. Kowalski [41a], C. Kozakai [157], W. Kozanecki [138], A.S. Kozhin [132], V.A. Kramarenko [101], G. Kramberger [78], D. Krasnopevtsev [100], M.W. Krasny [83], A. Krasznahorkay [32], D. Krauss [103], A. Kravchenko [27], J.A. Kremer [41a], M. Kretz [60c], J. Kretzschmar [77], K. Kreutzfeldt [55], P. Krieger [161], K. Krizka [33], K. Kroeninger [46], H. Kroha [103], J. Kroll [124], J. Kroseberg [23], J. Krstic [14], U. Kruchonak [68], H. Krüger [23], N. Krumnack [67], M.C. Kruse [48], M. Kruskal [24], T. Kubota [91], H. Kucuk [81], S. Kuday [4b], J.T. Kuechler [178], S. Kuehn [51], A. Kugel [60c], F. Kuger [177], T. Kuhl [45], V. Kukhtin [68], R. Kukla [88], Y. Kulchitsky [95], S. Kuleshov [34b], Y.P. Kulinich [169], M. Kuna [134a,134b], T. Kunigo [71], A. Kupco [129], O. Kuprash [155], H. Kurashige [70], L.L. Kurchaninov [163a], Y.A. Kurochkin [95], M.G. Kurth [35a], V. Kus [129], E.S. Kuwertz [172], M. Kuze [159], J. Kvita [117], T. Kwan [172], D. Kyriazopoulos [141], A. La Rosa [103], J.L. La Rosa Navarro [26d], L. La Rotonda [40a,40b], C. Lacasta [170], F. Lacava [134a,134b], J. Lacey [45], H. Lacker [17], D. Lacour [83], E. Ladygin [68], R. Lafaye [5], B. Laforge [83], T. Lagouri [179], S. Lai [57], S. Lammers [64], W. Lampl [7], E. Lançon [27], U. Landgraf [51], M.P.J. Landon [79], M.C. Lanfermann [52], V.S. Lang [60a], J.C. Lange [13], A.J. Lankford [166], F. Lanni [27], K. Lantzsch [23], A. Lanza [123a], A. Lapertosa [53a,53b], S. Laplace [83], J.F. Laporte [138], T. Lari [94a], F. Lasagni Manghi [22a,22b], M. Lassnig [32], P. Laurelli [50], W. Lavrijsen [16], A.T. Law [139], P. Laycock [77], T. Lazovich [59], M. Lazzaroni [94a,94b], B. Le [91], O. Le Dortz [83], E. Le Guirriec [88], E.P. Le Quilleuc [138], M. LeBlanc [172], T. LeCompte [6], F. Ledroit-Guillon [58], C.A. Lee [27], S.C. Lee [153], L. Lee [1], B. Lefebvre [90], G. Lefebvre [83], M. Lefebvre [172], F. Legger [102], C. Leggett [16], A. Lehan [77], G. Lehmann Miotto [32], X. Lei [7], W.A. Leight [45], A.G. Leister [179], M.A.L. Leite [26d], R. Leitner [131], D. Lellouch [175], B. Lemmer [57], K.J.C. Leney [81], T. Lenz [23], B. Lenzi [32], R. Leone [7], S. Leone [126a,126b], C. Leonidopoulos [49], G. Lerner [151], C. Leroy [97], A.A.J. Lesage [138], C.G. Lester [30], M. Levchenko [125], J. Levêque [5], D. Levin [92], L.J. Levinson [175], M. Levy [19], D. Lewis [79], B. Li [36a,s], Changqiao Li [36a], H. Li [150], L. Li [48], L. Li [36c], Q. Li [35a], S. Li [48], X. Li [36c], Y. Li [143], Z. Liang [35a], B. Liberti [135a], A. Liblong [161], K. Lie [169], J. Liebal [23], W. Liebig [15], A. Limosani [152], S.C. Lin [153,ag], T.H. Lin [86], B.E. Lindquist [150], A.E. Lionti [52], E. Lipeles [124], A. Lipniacka [15], M. Lisovyi [60b], T.M. Liss [169,ah], A. Lister [171], A.M. Litke [139], B. Liu [153,ai], H. Liu [92], H. Liu [27], J. Liu [36b], J.B. Liu [36a], K. Liu [88], L. Liu [169], M. Liu [36a], Y.L. Liu [36a], Y. Liu [36a], M. Livan [123a,123b], A. Lleres [58], J. Llorente Merino [35a], S.L. Lloyd [79], C.Y. Lo [62b], F. Lo Sterzo [153], E.M. Lobodzinska [45], P. Loch [7], F.K. Loebinger [87], K.M. Loew [25], A. Loginov [179,*], T. Lohse [17], K. Lohwasser [45], M. Lokajicek [129], B.A. Long [24], J.D. Long [169], R.E. Long [75], L. Longo [76a,76b], K.A. Looper [113], J.A. Lopez [34b], D. Lopez Mateos [59], I. Lopez Paz [13], A. Lopez Solis [83], J. Lorenz [102], N. Lorenzo Martinez [64], M. Losada [21], P.J. Lösel [102], X. Lou [35a], A. Lounis [119], J. Love [6], P.A. Love [75], H. Lu [62a], N. Lu [92], Y.J. Lu [63], H.J. Lubatti [140], C. Luci [134a,134b], A. Lucotte [58], C. Luedtke [51], F. Luehring [64], W. Lukas [65], L. Luminari [134a], O. Lundberg [148a,148b], B. Lund-Jensen [149], P.M. Luzi [83], D. Lynn [27], R. Lysak [129], E. Lytken [84], V. Lyubushkin [68], H. Ma [27], L.L. Ma [36b], Y. Ma [36b], G. Maccarrone [50], A. Macchiolo [103], C.M. Macdonald [141], B. Maček [78], J. Machado Miguens [124,128b], D. Madaffari [88], R. Madar [37], H.J. Maddocks [168], W.F. Mader [47], A. Madsen [45], J. Maeda [70], S. Maeland [15], T. Maeno [27], A.S. Maevskiy [101], E. Magradze [57], J. Mahlstedt [109], C. Maiani [119], C. Maidantchik [26a], A.A. Maier [103], T. Maier [102], A. Maio [128a,128b,128d], S. Majewski [118], Y. Makida [69], N. Makovec [119], B. Malaescu [83], Pa. Malecki [42], V.P. Maleev [125], F. Malek [58], U. Mallik [66], D. Malon [6], C. Malone [30], S. Maltezos [10], S. Malyukov [32], J. Mamuzic [170], G. Mancini [50], L. Mandelli [94a], I. Mandić [78], J. Maneira [128a,128b], L. Manhaes de Andrade Filho [26b], J. Manjarres Ramos [163b], A. Mann [102], A. Manousos [32], B. Mansoulie [138], J.D. Mansour [35a], R. Mantifel [90], M. Mantoani [57], S. Manzoni [94a,94b], L. Mapelli [32], G. Marceca [29], L. March [52], G. Marchiori [83], M. Marcisovsky [129], M. Marjanovic [37], D.E. Marley [92], F. Marroquim [26a], S.P. Marsden [87], Z. Marshall [16], M.U.F. Martensson [168], S. Marti-Garcia [170], C.B. Martin [113], T.A. Martin [173], V.J. Martin [49], B. Martin dit Latour [15], M. Martinez [13,w], V.I. Martinez Outschoorn [169], S. Martin-Haugh [133], V.S. Martoiu [28b], A.C. Martyniuk [81], A. Marzin [115], L. Masetti [86], T. Mashimo [157], R. Mashinistov [98], J. Masik [87], A.L. Maslennikov [111,c], L. Massa [135a,135b], P. Mastrandrea [5], A. Mastroberardino [40a,40b], T. Masubuchi [157], P. Mättig [178], J. Maurer [28b], S.J. Maxfield [77], D.A. Maximov [111,c], R. Mazini [153], I. Maznas [156], S.M. Mazza [94a,94b], N.C. Mc Fadden [107], G. Mc Goldrick [161], S.P. Mc Kee [92], A. McCarn [92],

R.L. McCarthy [150], T.G. McCarthy [103], L.I. McClymont [81], E.F. McDonald [91], J.A. Mcfayden [81], G. Mchedlidze [57], S.J. McMahon [133], P.C. McNamara [91], R.A. McPherson [172,o], S. Meehan [140], T.J. Megy [51], S. Mehlhase [102], A. Mehta [77], T. Meideck [58], K. Meier [60a], C. Meineck [102], B. Meirose [44], D. Melini [170,aj], B.R. Mellado Garcia [147c], M. Melo [146a], F. Meloni [18], S.B. Menary [87], L. Meng [77], X.T. Meng [92], A. Mengarelli [22a,22b], S. Menke [103], E. Meoni [165], S. Mergelmeyer [17], P. Mermod [52], L. Merola [106a,106b], C. Meroni [94a], F.S. Merritt [33], A. Messina [134a,134b], J. Metcalfe [6], A.S. Mete [166], C. Meyer [124], J-P. Meyer [138], J. Meyer [109], H. Meyer Zu Theenhausen [60a], F. Miano [151], R.P. Middleton [133], S. Miglioranzi [53a,53b], L. Mijović [49], G. Mikenberg [175], M. Mikestikova [129], M. Mikuž [78], M. Milesi [91], A. Milic [27], D.W. Miller [33], C. Mills [49], A. Milov [175], D.A. Milstead [148a,148b], A.A. Minaenko [132], Y. Minami [157], I.A. Minashvili [68], A.I. Mincer [112], B. Mindur [41a], M. Mineev [68], Y. Minegishi [157], Y. Ming [176], L.M. Mir [13], K.P. Mistry [124], T. Mitani [174], J. Mitrevski [102], V.A. Mitsou [170], A. Miucci [18], P.S. Miyagawa [141], A. Mizukami [69], J.U. Mjörnmark [84], M. Mlynarikova [131], T. Moa [148a,148b], K. Mochizuki [97], P. Mogg [51], S. Mohapatra [38], S. Molander [148a,148b], R. Moles-Valls [23], R. Monden [71], M.C. Mondragon [93], K. Mönig [45], J. Monk [39], E. Monnier [88], A. Montalbano [150], J. Montejo Berlingen [32], F. Monticelli [74], S. Monzani [94a,94b], R.W. Moore [3], N. Morange [119], D. Moreno [21], M. Moreno Llácer [57], P. Morettini [53a], S. Morgenstern [32], D. Mori [144], T. Mori [157], M. Morii [59], M. Morinaga [157], V. Morisbak [121], A.K. Morley [152], G. Mornacchi [32], J.D. Morris [79], L. Morvaj [150], P. Moschovakos [10], M. Mosidze [54b], H.J. Moss [141], J. Moss [145,ak], K. Motohashi [159], R. Mount [145], E. Mountricha [27], E.J.W. Moyse [89], S. Muanza [88], R.D. Mudd [19], F. Mueller [103], J. Mueller [127], R.S.P. Mueller [102], D. Muenstermann [75], P. Mullen [56], G.A. Mullier [18], F.J. Munoz Sanchez [87], W.J. Murray [173,133], H. Musheghyan [57], M. Muškinja [78], A.G. Myagkov [132,al], M. Myska [130], B.P. Nachman [16], O. Nackenhorst [52], K. Nagai [122], R. Nagai [69,ae], K. Nagano [69], Y. Nagasaka [61], K. Nagata [164], M. Nagel [51], E. Nagy [88], A.M. Nairz [32], Y. Nakahama [105], K. Nakamura [69], T. Nakamura [157], I. Nakano [114], R.F. Naranjo Garcia [45], R. Narayan [11], D.I. Narrias Villar [60a], I. Naryshkin [125], T. Naumann [45], G. Navarro [21], R. Nayyar [7], H.A. Neal [92], P.Yu. Nechaeva [98], T.J. Neep [138], A. Negri [123a,123b], M. Negrini [22a], S. Nektarijevic [108], C. Nellist [119], A. Nelson [166], S. Nemecek [129], P. Nemethy [112], A.A. Nepomuceno [26a], M. Nessi [32,am], M.S. Neubauer [169], M. Neumann [178], R.M. Neves [112], P. Nevski [27], P.R. Newman [19], T.Y. Ng [62c], T. Nguyen Manh [97], R.B. Nickerson [122], R. Nicolaidou [138], J. Nielsen [139], V. Nikolaenko [132,al], I. Nikolic-Audit [83], K. Nikolopoulos [19], J.K. Nilsen [121], P. Nilsson [27], Y. Ninomiya [157], A. Nisati [134a], N. Nishu [35c], R. Nisius [103], T. Nobe [157], Y. Noguchi [71], M. Nomachi [120], I. Nomidis [31], M.A. Nomura [27], T. Nooney [79], M. Nordberg [32], N. Norjoharuddeen [122], O. Novgorodova [47], S. Nowak [103], M. Nozaki [69], L. Nozka [117], K. Ntekas [166], E. Nurse [81], F. Nuti [91], D.C. O'Neil [144], A.A. O'Rourke [45], V. O'Shea [56], F.G. Oakham [31,d], H. Oberlack [103], T. Obermann [23], J. Ocariz [83], A. Ochi [70], I. Ochoa [38], J.P. Ochoa-Ricoux [34a], S. Oda [73], S. Odaka [69], H. Ogren [64], A. Oh [87], S.H. Oh [48], C.C. Ohm [16], H. Ohman [168], H. Oide [53a,53b], H. Okawa [164], Y. Okumura [157], T. Okuyama [69], A. Olariu [28b], L.F. Oleiro Seabra [128a], S.A. Olivares Pino [49], D. Oliveira Damazio [27], A. Olszewski [42], J. Olszowska [42], A. Onofre [128a,128e], K. Onogi [105], P.U.E. Onyisi [11,aa], M.J. Oreglia [33], Y. Oren [155], D. Orestano [136a,136b], N. Orlando [62b], R.S. Orr [161], B. Osculati [53a,53b,*], R. Ospanov [87], G. Otero y Garzon [29], H. Otono [73], M. Ouchrif [137d], F. Ould-Saada [121], A. Ouraou [138], K.P. Oussoren [109], Q. Ouyang [35a], M. Owen [56], R.E. Owen [19], V.E. Ozcan [20a], N. Ozturk [8], K. Pachal [144], A. Pacheco Pages [13], L. Pacheco Rodriguez [138], C. Padilla Aranda [13], S. Pagan Griso [16], M. Paganini [179], F. Paige [27], P. Pais [89], G. Palacino [64], S. Palazzo [40a,40b], S. Palestini [32], M. Palka [41b], D. Pallin [37], E. St. Panagiotopoulou [10], I. Panagoulias [10], C.E. Pandini [83], J.G. Panduro Vazquez [80], P. Pani [32], S. Panitkin [27], D. Pantea [28b], L. Paolozzi [52], Th.D. Papadopoulou [10], K. Papageorgiou [9,t], A. Paramonov [6], D. Paredes Hernandez [179], A.J. Parker [75], M.A. Parker [30], K.A. Parker [45], F. Parodi [53a,53b], J.A. Parsons [38], U. Parzefall [51], V.R. Pascuzzi [161], J.M. Pasner [139], E. Pasqualucci [134a], S. Passaggio [53a], Fr. Pastore [80], S. Pataraia [178], J.R. Pater [87], T. Pauly [32], J. Pearce [172], B. Pearson [103], L.E. Pedersen [39], S. Pedraza Lopez [170], R. Pedro [128a,128b], S.V. Peleganchuk [111,c], O. Penc [129], C. Peng [35a], H. Peng [36a], J. Penwell [64], B.S. Peralva [26b], M.M. Perego [138], D.V. Perepelitsa [27], L. Perini [94a,94b], H. Pernegger [32], S. Perrella [106a,106b], R. Peschke [45], V.D. Peshekhonov [68,*], K. Peters [45], R.F.Y. Peters [87], B.A. Petersen [32], T.C. Petersen [39], E. Petit [58], A. Petridis [1], C. Petridou [156], P. Petroff [119], E. Petrolo [134a], M. Petrov [122], F. Petrucci [136a,136b], N.E. Pettersson [89], A. Peyaud [138], R. Pezoa [34b], P.W. Phillips [133], G. Piacquadio [150], E. Pianori [173], A. Picazio [89], E. Piccaro [79], M.A. Pickering [122], R. Piegaia [29], J.E. Pilcher [33], A.D. Pilkington [87], A.W.J. Pin [87], M. Pinamonti [167a,167c,an], J.L. Pinfold [3], H. Pirumov [45], M. Pitt [175], L. Plazak [146a], M.-A. Pleier [27],

V. Pleskot [86], E. Plotnikova [68], D. Pluth [67], P. Podberezko [111], R. Poettgen [148a,148b], L. Poggioli [119], D. Pohl [23], G. Polesello [123a], A. Poley [45], A. Policicchio [40a,40b], R. Polifka [32], A. Polini [22a], C.S. Pollard [56], V. Polychronakos [27], K. Pommès [32], L. Pontecorvo [134a], B.G. Pope [93], G.A. Popeneciu [28d], A. Poppleton [32], S. Pospisil [130], K. Potamianos [16], I.N. Potrap [68], C.J. Potter [30], G. Poulard [32], J. Poveda [32], M.E. Pozo Astigarraga [32], P. Pralavorio [88], A. Pranko [16], S. Prell [67], D. Price [87], L.E. Price [6], M. Primavera [76a], S. Prince [90], K. Prokofiev [62c], F. Prokoshin [34b], S. Protopopescu [27], J. Proudfoot [6], M. Przybycien [41a], D. Puddu [136a,136b], A. Puri [169], P. Puzo [119], J. Qian [92], G. Qin [56], Y. Qin [87], A. Quadt [57], M. Queitsch-Maitland [45], D. Quilty [56], S. Raddum [121], V. Radeka [27], V. Radescu [122], S.K. Radhakrishnan [150], P. Radloff [118], P. Rados [91], F. Ragusa [94a,94b], G. Rahal [181], J.A. Raine [87], S. Rajagopalan [27], C. Rangel-Smith [168], M.G. Ratti [94a,94b], D.M. Rauch [45], F. Rauscher [102], S. Rave [86], T. Ravenscroft [56], I. Ravinovich [175], M. Raymond [32], A.L. Read [121], N.P. Readioff [77], M. Reale [76a,76b], D.M. Rebuzzi [123a,123b], A. Redelbach [177], G. Redlinger [27], R. Reece [139], R.G. Reed [147c], K. Reeves [44], L. Rehnisch [17], J. Reichert [124], A. Reiss [86], C. Rembser [32], H. Ren [35a], M. Rescigno [134a], S. Resconi [94a], E.D. Resseguie [124], S. Rettie [171], E. Reynolds [19], O.L. Rezanova [111,c], P. Reznicek [131], R. Rezvani [97], R. Richter [103], S. Richter [81], E. Richter-Was [41b], O. Ricken [23], M. Ridel [83], P. Rieck [103], C.J. Riegel [178], J. Rieger [57], O. Rifki [115], M. Rijssenbeek [150], A. Rimoldi [123a,123b], M. Rimoldi [18], L. Rinaldi [22a], B. Ristić [52], E. Ritsch [32], I. Riu [13], F. Rizatdinova [116], E. Rizvi [79], C. Rizzi [13], R.T. Roberts [87], S.H. Robertson [90,o], A. Robichaud-Veronneau [90], D. Robinson [30], J.E.M. Robinson [45], A. Robson [56], C. Roda [126a,126b], Y. Rodina [88,ao], A. Rodriguez Perez [13], D. Rodriguez Rodriguez [170], S. Roe [32], C.S. Rogan [59], O. Røhne [121], J. Roloff [59], A. Romaniouk [100], M. Romano [22a,22b], S.M. Romano Saez [37], E. Romero Adam [170], N. Rompotis [77], M. Ronzani [51], L. Roos [83], S. Rosati [134a], K. Rosbach [51], P. Rose [139], N.-A. Rosien [57], V. Rossetti [148a,148b], E. Rossi [106a,106b], L.P. Rossi [53a], J.H.N. Rosten [30], R. Rosten [140], M. Rotaru [28b], I. Roth [175], J. Rothberg [140], D. Rousseau [119], A. Rozanov [88], Y. Rozen [154], X. Ruan [147c], F. Rubbo [145], F. Rühr [51], A. Ruiz-Martinez [31], Z. Rurikova [51], N.A. Rusakovich [68], A. Ruschke [102], H.L. Russell [140], J.P. Rutherfoord [7], N. Ruthmann [32], Y.F. Ryabov [125], M. Rybar [169], G. Rybkin [119], S. Ryu [6], A. Ryzhov [132], G.F. Rzehorz [57], A.F. Saavedra [152], G. Sabato [109], S. Sacerdoti [29], H.F.-W. Sadrozinski [139], R. Sadykov [68], F. Safai Tehrani [134a], P. Saha [110], M. Sahinsoy [60a], M. Saimpert [45], T. Saito [157], H. Sakamoto [157], Y. Sakurai [174], G. Salamanna [136a,136b], J.E. Salazar Loyola [34b], D. Salek [109], P.H. Sales De Bruin [140], D. Salihagic [103], A. Salnikov [145], J. Salt [170], D. Salvatore [40a,40b], F. Salvatore [151], A. Salvucci [62a,62b,62c], A. Salzburger [32], D. Sammel [51], D. Sampsonidis [156], J. Sánchez [170], V. Sanchez Martinez [170], A. Sanchez Pineda [106a,106b], H. Sandaker [121], R.L. Sandbach [79], C.O. Sander [45], M. Sandhoff [178], C. Sandoval [21], D.P.C. Sankey [133], M. Sannino [53a,53b], A. Sansoni [50], C. Santoni [37], R. Santonico [135a,135b], H. Santos [128a], I. Santoyo Castillo [151], K. Sapp [127], A. Sapronov [68], J.G. Saraiva [128a,128d], B. Sarrazin [23], O. Sasaki [69], K. Sato [164], E. Sauvan [5], G. Savage [80], P. Savard [161,d], N. Savic [103], C. Sawyer [133], L. Sawyer [82,v], J. Saxon [33], C. Sbarra [22a], A. Sbrizzi [22a,22b], T. Scanlon [81], D.A. Scannicchio [166], M. Scarcella [152], V. Scarfone [40a,40b], J. Schaarschmidt [140], P. Schacht [103], B.M. Schachtner [102], D. Schaefer [32], L. Schaefer [124], R. Schaefer [45], J. Schaeffer [86], S. Schaepe [23], S. Schaetzel [60b], U. Schäfer [86], A.C. Schaffer [119], D. Schaile [102], R.D. Schamberger [150], V. Scharf [60a], V.A. Schegelsky [125], D. Scheirich [131], M. Schernau [166], C. Schiavi [53a,53b], S. Schier [139], C. Schillo [51], M. Schioppa [40a,40b], S. Schlenker [32], K.R. Schmidt-Sommerfeld [103], K. Schmieden [32], C. Schmitt [86], S. Schmitt [45], S. Schmitz [86], B. Schneider [163a], U. Schnoor [51], L. Schoeffel [138], A. Schoening [60b], B.D. Schoenrock [93], E. Schopf [23], M. Schott [86], J.F.P. Schouwenberg [108], J. Schovancova [8], S. Schramm [52], N. Schuh [86], A. Schulte [86], M.J. Schultens [23], H.-C. Schultz-Coulon [60a], H. Schulz [17], M. Schumacher [51], B.A. Schumm [139], Ph. Schune [138], A. Schwartzman [145], T.A. Schwarz [92], H. Schweiger [87], Ph. Schwemling [138], R. Schwienhorst [93], J. Schwindling [138], T. Schwindt [23], G. Sciolla [25], F. Scuri [126a,126b], F. Scutti [91], J. Searcy [92], P. Seema [23], S.C. Seidel [107], A. Seiden [139], J.M. Seixas [26a], G. Sekhniaidze [106a], K. Sekhon [92], S.J. Sekula [43], N. Semprini-Cesari [22a,22b], C. Serfon [121], L. Serin [119], L. Serkin [167a,167b], M. Sessa [136a,136b], R. Seuster [172], H. Severini [115], T. Sfiligoj [78], F. Sforza [32], A. Sfyrla [52], E. Shabalina [57], N.W. Shaikh [148a,148b], L.Y. Shan [35a], R. Shang [169], J.T. Shank [24], M. Shapiro [16], P.B. Shatalov [99], K. Shaw [167a,167b], S.M. Shaw [87], A. Shcherbakova [148a,148b], C.Y. Shehu [151], Y. Shen [115], P. Sherwood [81], L. Shi [153,ap], S. Shimizu [70], C.O. Shimmin [179], M. Shimojima [104], S. Shirabe [73], M. Shiyakova [68,aq], J. Shlomi [175], A. Shmeleva [98], D. Shoaleh Saadi [97], M.J. Shochet [33], S. Shojaii [94a], D.R. Shope [115], S. Shrestha [113], E. Shulga [100], M.A. Shupe [7], P. Sicho [129], A.M. Sickles [169], P.E. Sidebo [149],

E. Sideras Haddad [147c], O. Sidiropoulou [177], D. Sidorov [116], A. Sidoti [22a,22b], F. Siegert [47], Dj. Sijacki [14], J. Silva [128a,128d], S.B. Silverstein [148a], V. Simak [130], Lj. Simic [14], S. Simion [119], E. Simioni [86], B. Simmons [81], M. Simon [86], P. Sinervo [161], N.B. Sinev [118], M. Sioli [22a,22b], G. Siragusa [177], I. Siral [92], S.Yu. Sivoklokov [101], J. Sjölin [148a,148b], M.B. Skinner [75], P. Skubic [115], M. Slater [19], T. Slavicek [130], M. Slawinska [109], K. Sliwa [165], R. Slovak [131], V. Smakhtin [175], B.H. Smart [5], L. Smestad [15], J. Smiesko [146a], S.Yu. Smirnov [100], Y. Smirnov [100], L.N. Smirnova [101,ar], O. Smirnova [84], J.W. Smith [57], M.N.K. Smith [38], R.W. Smith [38], M. Smizanska [75], K. Smolek [130], A.A. Snesarev [98], I.M. Snyder [118], S. Snyder [27], R. Sobie [172,o], F. Socher [47], A. Soffer [155], D.A. Soh [153], G. Sokhrannyi [78], C.A. Solans Sanchez [32], M. Solar [130], E.Yu. Soldatov [100], U. Soldevila [170], A.A. Solodkov [132], A. Soloshenko [68], O.V. Solovyanov [132], V. Solovyev [125], P. Sommer [51], H. Son [165], H.Y. Song [36a,as], A. Sopczak [130], V. Sorin [13], D. Sosa [60b], C.L. Sotiropoulou [126a,126b], R. Soualah [167a,167c], A.M. Soukharev [111,c], D. South [45], B.C. Sowden [80], S. Spagnolo [76a,76b], M. Spalla [126a,126b], M. Spangenberg [173], F. Spanò [80], D. Sperlich [17], F. Spettel [103], T.M. Spieker [60a], R. Spighi [22a], G. Spigo [32], L.A. Spiller [91], M. Spousta [131], R.D. St. Denis [56,*], A. Stabile [94a], R. Stamen [60a], S. Stamm [17], E. Stanecka [42], R.W. Stanek [6], C. Stanescu [136a], M.M. Stanitzki [45], S. Stapnes [121], E.A. Starchenko [132], G.H. Stark [33], J. Stark [58], S.H. Stark [39], P. Staroba [129], P. Starovoitov [60a], S. Stärz [32], R. Staszewski [42], P. Steinberg [27], B. Stelzer [144], H.J. Stelzer [32], O. Stelzer-Chilton [163a], H. Stenzel [55], G.A. Stewart [56], J.A. Stillings [23], M.C. Stockton [90], M. Stoebe [90], G. Stoicea [28b], P. Stolte [57], S. Stonjek [103], A.R. Stradling [8], A. Straessner [47], M.E. Stramaglia [18], J. Strandberg [149], S. Strandberg [148a,148b], A. Strandlie [121], M. Strauss [115], P. Strizenec [146b], R. Ströhmer [177], D.M. Strom [118], R. Stroynowski [43], A. Strubig [108], S.A. Stucci [27], B. Stugu [15], N.A. Styles [45], D. Su [145], J. Su [127], S. Suchek [60a], Y. Sugaya [120], M. Suk [130], V.V. Sulin [98], S. Sultansoy [4c], T. Sumida [71], S. Sun [59], X. Sun [3], K. Suruliz [151], C.J.E. Suster [152], M.R. Sutton [151], S. Suzuki [69], M. Svatos [129], M. Swiatlowski [33], S.P. Swift [2], I. Sykora [146a], T. Sykora [131], D. Ta [51], K. Tackmann [45], J. Taenzer [155], A. Taffard [166], R. Tafirout [163a], N. Taiblum [155], H. Takai [27], R. Takashima [72], T. Takeshita [142], Y. Takubo [69], M. Talby [88], A.A. Talyshev [111,c], J. Tanaka [157], M. Tanaka [159], R. Tanaka [119], S. Tanaka [69], R. Tanioka [70], B.B. Tannenwald [113], S. Tapia Araya [34b], S. Tapprogge [86], S. Tarem [154], G.F. Tartarelli [94a], P. Tas [131], M. Tasevsky [129], T. Tashiro [71], E. Tassi [40a,40b], A. Tavares Delgado [128a,128b], Y. Tayalati [137e], A.C. Taylor [107], G.N. Taylor [91], P.T.E. Taylor [91], W. Taylor [163b], P. Teixeira-Dias [80], D. Temple [144], H. Ten Kate [32], P.K. Teng [153], J.J. Teoh [120], F. Tepel [178], S. Terada [69], K. Terashi [157], J. Terron [85], S. Terzo [13], M. Testa [50], R.J. Teuscher [161,o], T. Theveneaux-Pelzer [88], J.P. Thomas [19], J. Thomas-Wilsker [80], P.D. Thompson [19], A.S. Thompson [56], L.A. Thomsen [179], E. Thomson [124], M.J. Tibbetts [16], R.E. Ticse Torres [88], V.O. Tikhomirov [98,at], Yu.A. Tikhonov [111,c], S. Timoshenko [100], P. Tipton [179], S. Tisserant [88], K. Todome [159], S. Todorova-Nova [5], J. Tojo [73], S. Tokár [146a], K. Tokushuku [69], E. Tolley [59], L. Tomlinson [87], M. Tomoto [105], L. Tompkins [145,au], K. Toms [107], B. Tong [59], P. Tornambe [51], E. Torrence [118], H. Torres [144], E. Torró Pastor [140], J. Toth [88,av], F. Touchard [88], D.R. Tovey [141], C.J. Treado [112], T. Trefzger [177], A. Tricoli [27], I.M. Trigger [163a], S. Trincaz-Duvoid [83], M.F. Tripiana [13], W. Trischuk [161], B. Trocmé [58], A. Trofymov [45], C. Troncon [94a], M. Trottier-McDonald [16], M. Trovatelli [172], L. Truong [167a,167c], M. Trzebinski [42], A. Trzupek [42], K.W. Tsang [62a], J.C.-L. Tseng [122], P.V. Tsiareshka [95], G. Tsipolitis [10], N. Tsirintanis [9], S. Tsiskaridze [13], V. Tsiskaridze [51], E.G. Tskhadadze [54a], K.M. Tsui [62a], I.I. Tsukerman [99], V. Tsulaia [16], S. Tsuno [69], D. Tsybychev [150], Y. Tu [62b], A. Tudorache [28b], V. Tudorache [28b], T.T. Tulbure [28a], A.N. Tuna [59], S.A. Tupputi [22a,22b], S. Turchikhin [68], D. Turgeman [175], I. Turk Cakir [4b,aw], R. Turra [94a], P.M. Tuts [38], G. Ucchielli [22a,22b], I. Ueda [69], M. Ughetto [148a,148b], F. Ukegawa [164], G. Unal [32], A. Undrus [27], G. Unel [166], F.C. Ungaro [91], Y. Unno [69], C. Unverdorben [102], J. Urban [146b], P. Urquijo [91], P. Urrejola [86], G. Usai [8], J. Usui [69], L. Vacavant [88], V. Vacek [130], B. Vachon [90], C. Valderanis [102], E. Valdes Santurio [148a,148b], N. Valencic [109], S. Valentinetti [22a,22b], A. Valero [170], L. Valéry [13], S. Valkar [131], A. Vallier [5], J.A. Valls Ferrer [170], W. Van Den Wollenberg [109], H. van der Graaf [109], N. van Eldik [154], P. van Gemmeren [6], J. Van Nieuwkoop [144], I. van Vulpen [109], M.C. van Woerden [109], M. Vanadia [134a,134b], W. Vandelli [32], R. Vanguri [124], A. Vaniachine [160], P. Vankov [109], G. Vardanyan [180], R. Vari [134a], E.W. Varnes [7], C. Varni [53a,53b], T. Varol [43], D. Varouchas [83], A. Vartapetian [8], K.E. Varvell [152], J.G. Vasquez [179], G.A. Vasquez [34b], F. Vazeille [37], T. Vazquez Schroeder [90], J. Veatch [57], V. Veeraraghavan [7], L.M. Veloce [161], F. Veloso [128a,128c], S. Veneziano [134a], A. Ventura [76a,76b], M. Venturi [172], N. Venturi [161], A. Venturini [25], V. Vercesi [123a], M. Verducci [136a,136b], W. Verkerke [109], J.C. Vermeulen [109], M.C. Vetterli [144,d], N. Viaux Maira [34a], O. Viazlo [84], I. Vichou [169,*], T. Vickey [141], O.E. Vickey Boeriu [141],

G.H.A. Viehhauser [122], S. Viel [16], L. Vigani [122], M. Villa [22a,22b], M. Villaplana Perez [94a,94b], E. Vilucchi [50], M.G. Vincter [31], V.B. Vinogradov [68], A. Vishwakarma [45], C. Vittori [22a,22b], I. Vivarelli [151], S. Vlachos [10], M. Vlasak [130], M. Vogel [178], P. Vokac [130], G. Volpi [126a,126b], H. von der Schmitt [103], E. von Toerne [23], V. Vorobel [131], K. Vorobev [100], M. Vos [170], R. Voss [32], J.H. Vossebeld [77], N. Vranjes [14], M. Vranjes Milosavljevic [14], V. Vrba [130], M. Vreeswijk [109], R. Vuillermet [32], I. Vukotic [33], P. Wagner [23], W. Wagner [178], H. Wahlberg [74], S. Wahrmund [47], J. Wakabayashi [105], J. Walder [75], R. Walker [102], W. Walkowiak [143], V. Wallangen [148a,148b], C. Wang [35b], C. Wang [36b,ax], F. Wang [176], H. Wang [16], H. Wang [3], J. Wang [45], J. Wang [152], Q. Wang [115], R. Wang [6], S.M. Wang [153], T. Wang [38], W. Wang [153,ay], W. Wang [36a], C. Wanotayaroj [118], A. Warburton [90], C.P. Ward [30], D.R. Wardrope [81], A. Washbrook [49], P.M. Watkins [19], A.T. Watson [19], M.F. Watson [19], G. Watts [140], S. Watts [87], B.M. Waugh [81], A.F. Webb [11], S. Webb [86], M.S. Weber [18], S.W. Weber [177], S.A. Weber [31], J.S. Webster [6], A.R. Weidberg [122], B. Weinert [64], J. Weingarten [57], C. Weiser [51], H. Weits [109], P.S. Wells [32], T. Wenaus [27], T. Wengler [32], S. Wenig [32], N. Wermes [23], M.D. Werner [67], P. Werner [32], M. Wessels [60a], K. Whalen [118], N.L. Whallon [140], A.M. Wharton [75], A. White [8], M.J. White [1], R. White [34b], D. Whiteson [166], F.J. Wickens [133], W. Wiedenmann [176], M. Wielers [133], C. Wiglesworth [39], L.A.M. Wiik-Fuchs [23], A. Wildauer [103], F. Wilk [87], H.G. Wilkens [32], H.H. Williams [124], S. Williams [109], C. Willis [93], S. Willocq [89], J.A. Wilson [19], I. Wingerter-Seez [5], F. Winklmeier [118], O.J. Winston [151], B.T. Winter [23], M. Wittgen [145], M. Wobisch [82,v], T.M.H. Wolf [109], R. Wolff [88], M.W. Wolter [42], H. Wolters [128a,128c], S.D. Worm [19], B.K. Wosiek [42], J. Wotschack [32], M.J. Woudstra [87], K.W. Wozniak [42], M. Wu [33], S.L. Wu [176], X. Wu [52], Y. Wu [92], T.R. Wyatt [87], B.M. Wynne [49], S. Xella [39], Z. Xi [92], L. Xia [35c], D. Xu [35a], L. Xu [27], B. Yabsley [152], S. Yacoob [147a], D. Yamaguchi [159], Y. Yamaguchi [120], A. Yamamoto [69], S. Yamamoto [157], T. Yamanaka [157], K. Yamauchi [105], Y. Yamazaki [70], Z. Yan [24], H. Yang [36c], H. Yang [16], Y. Yang [153], Z. Yang [15], W-M. Yao [16], Y.C. Yap [83], Y. Yasu [69], E. Yatsenko [5], K.H. Yau Wong [23], J. Ye [43], S. Ye [27], I. Yeletskikh [68], E. Yildirim [86], K. Yorita [174], K. Yoshihara [124], C. Young [145], C.J.S. Young [32], S. Youssef [24], D.R. Yu [16], J. Yu [8], J. Yu [67], L. Yuan [70], S.P.Y. Yuen [23], I. Yusuff [30,az], B. Zabinski [42], G. Zacharis [10], R. Zaidan [13], A.M. Zaitsev [132,al], N. Zakharchuk [45], J. Zalieckas [15], A. Zaman [150], S. Zambito [59], D. Zanzi [91], C. Zeitnitz [178], M. Zeman [130], A. Zemla [41a], J.C. Zeng [169], Q. Zeng [145], O. Zenin [132], T. Ženiš [146a], D. Zerwas [119], D. Zhang [92], F. Zhang [176], G. Zhang [36a,as], H. Zhang [35b], J. Zhang [6], L. Zhang [51], L. Zhang [36a], M. Zhang [169], R. Zhang [23], R. Zhang [36a,ax], X. Zhang [36b], Y. Zhang [35a], Z. Zhang [119], X. Zhao [43], Y. Zhao [36b,ba], Z. Zhao [36a], A. Zhemchugov [68], J. Zhong [122], B. Zhou [92], C. Zhou [176], L. Zhou [43], M. Zhou [35a], M. Zhou [150], N. Zhou [35c], C.G. Zhu [36b], H. Zhu [35a], J. Zhu [92], Y. Zhu [36a], X. Zhuang [35a], K. Zhukov [98], A. Zibell [177], D. Zieminska [64], N.I. Zimine [68], C. Zimmermann [86], S. Zimmermann [51], Z. Zinonos [103], M. Zinser [86], M. Ziolkowski [143], L. Živković [14], G. Zobernig [176], A. Zoccoli [22a,22b], R. Zou [33], M. zur Nedden [17], L. Zwalinski [32]

[1] *Department of Physics, University of Adelaide, Adelaide, Australia*
[2] *Physics Department, SUNY Albany, Albany NY, United States*
[3] *Department of Physics, University of Alberta, Edmonton AB, Canada*
[4] [(a)] *Department of Physics, Ankara University, Ankara;* [(b)] *Istanbul Aydin University, Istanbul;* [(c)] *Division of Physics, TOBB University of Economics and Technology, Ankara, Turkey*
[5] *LAPP, CNRS/IN2P3 and Université Savoie Mont Blanc, Annecy-le-Vieux, France*
[6] *High Energy Physics Division, Argonne National Laboratory, Argonne IL, United States*
[7] *Department of Physics, University of Arizona, Tucson AZ, United States*
[8] *Department of Physics, The University of Texas at Arlington, Arlington TX, United States*
[9] *Physics Department, National and Kapodistrian University of Athens, Athens, Greece*
[10] *Physics Department, National Technical University of Athens, Zografou, Greece*
[11] *Department of Physics, The University of Texas at Austin, Austin TX, United States*
[12] *Institute of Physics, Azerbaijan Academy of Sciences, Baku, Azerbaijan*
[13] *Institut de Física d'Altes Energies (IFAE), The Barcelona Institute of Science and Technology, Barcelona, Spain*
[14] *Institute of Physics, University of Belgrade, Belgrade, Serbia*
[15] *Department for Physics and Technology, University of Bergen, Bergen, Norway*
[16] *Physics Division, Lawrence Berkeley National Laboratory and University of California, Berkeley CA, United States*
[17] *Department of Physics, Humboldt University, Berlin, Germany*
[18] *Albert Einstein Center for Fundamental Physics and Laboratory for High Energy Physics, University of Bern, Bern, Switzerland*
[19] *School of Physics and Astronomy, University of Birmingham, Birmingham, United Kingdom*
[20] [(a)] *Department of Physics, Bogazici University, Istanbul;* [(b)] *Department of Physics Engineering, Gaziantep University, Gaziantep;* [(c)] *Istanbul Bilgi University, Faculty of Engineering and Natural Sciences, Istanbul;* [(d)] *Bahcesehir University, Faculty of Engineering and Natural Sciences, Istanbul, Turkey*
[21] *Centro de Investigaciones, Universidad Antonio Narino, Bogota, Colombia*
[22] [(a)] *INFN Sezione di Bologna;* [(b)] *Dipartimento di Fisica e Astronomia, Università di Bologna, Bologna, Italy*
[23] *Physikalisches Institut, University of Bonn, Bonn, Germany*
[24] *Department of Physics, Boston University, Boston MA, United States*
[25] *Department of Physics, Brandeis University, Waltham MA, United States*
[26] [(a)] *Universidade Federal do Rio De Janeiro COPPE/EE/IF, Rio de Janeiro;* [(b)] *Electrical Circuits Department, Federal University of Juiz de Fora (UFJF), Juiz de Fora;* [(c)] *Federal University of Sao Joao del Rei (UFSJ), Sao Joao del Rei;* [(d)] *Instituto de Fisica, Universidade de Sao Paulo, Sao Paulo, Brazil*

[27] Physics Department, Brookhaven National Laboratory, Upton NY, United States
[28] [(a)] Transilvania University of Brasov, Brasov; [(b)] Horia Hulubei National Institute of Physics and Nuclear Engineering, Bucharest; [(c)] Department of Physics, Alexandru Ioan Cuza University of Iasi, Iasi; [(d)] National Institute for Research and Development of Isotopic and Molecular Technologies, Physics Department, Cluj Napoca; [(e)] University Politehnica Bucharest, Bucharest; [(f)] West University in Timisoara, Timisoara, Romania
[29] Departamento de Física, Universidad de Buenos Aires, Buenos Aires, Argentina
[30] Cavendish Laboratory, University of Cambridge, Cambridge, United Kingdom
[31] Department of Physics, Carleton University, Ottawa ON, Canada
[32] CERN, Geneva, Switzerland
[33] Enrico Fermi Institute, University of Chicago, Chicago IL, United States
[34] [(a)] Departamento de Física, Pontificia Universidad Católica de Chile, Santiago; [(b)] Departamento de Física, Universidad Técnica Federico Santa María, Valparaíso, Chile
[35] [(a)] Institute of High Energy Physics, University of CAS, Chinese Academy of Sciences, Beijing; [(b)] Department of Physics, Nanjing University, Jiangsu; [(c)] Physics Department, Tsinghua University, Beijing 100084, China
[36] [(a)] Department of Modern Physics and State Key Laboratory of Particle Detection and Electronics, University of Science and Technology of China, Anhui, China; [(b)] School of Physics, Shandong University, Shandong, China; [(c)] Department of Physics and Astronomy, Key Laboratory for Particle Physics, Astrophysics and Cosmology, Ministry of Education, Shanghai Key Laboratory for Particle Physics and Cosmology, Shanghai Jiao Tong University, Shanghai, China [bb]
[37] Université Clermont Auvergne, CNRS/IN2P3, LPC, Clermont-Ferrand, France
[38] Nevis Laboratory, Columbia University, Irvington NY, United States
[39] Niels Bohr Institute, University of Copenhagen, Kobenhavn, Denmark
[40] [(a)] INFN Gruppo Collegato di Cosenza, Laboratori Nazionali di Frascati; [(b)] Dipartimento di Fisica, Università della Calabria, Rende, Italy
[41] [(a)] AGH University of Science and Technology, Faculty of Physics and Applied Computer Science, Krakow; [(b)] Marian Smoluchowski Institute of Physics, Jagiellonian University, Krakow, Poland
[42] Institute of Nuclear Physics Polish Academy of Sciences, Krakow, Poland
[43] Physics Department, Southern Methodist University, Dallas TX, United States
[44] Physics Department, University of Texas at Dallas, Richardson TX, United States
[45] DESY, Hamburg and Zeuthen, Germany
[46] Lehrstuhl für Experimentelle Physik IV, Technische Universität Dortmund, Dortmund, Germany
[47] Institut für Kern- und Teilchenphysik, Technische Universität Dresden, Dresden, Germany
[48] Department of Physics, Duke University, Durham NC, United States
[49] SUPA – School of Physics and Astronomy, University of Edinburgh, Edinburgh, United Kingdom
[50] INFN e Laboratori Nazionali di Frascati, Frascati, Italy
[51] Fakultät für Mathematik und Physik, Albert-Ludwigs-Universität, Freiburg, Germany
[52] Departement de Physique Nucleaire et Corpusculaire, Université de Genève, Geneva, Switzerland
[53] [(a)] INFN Sezione di Genova; [(b)] Dipartimento di Fisica, Università di Genova, Genova, Italy
[54] [(a)] E. Andronikashvili Institute of Physics, Iv. Javakhishvili Tbilisi State University, Tbilisi; [(b)] High Energy Physics Institute, Tbilisi State University, Tbilisi, Georgia
[55] II Physikalisches Institut, Justus-Liebig-Universität Giessen, Giessen, Germany
[56] SUPA – School of Physics and Astronomy, University of Glasgow, Glasgow, United Kingdom
[57] II Physikalisches Institut, Georg-August-Universität, Göttingen, Germany
[58] Laboratoire de Physique Subatomique et de Cosmologie, Université Grenoble-Alpes, CNRS/IN2P3, Grenoble, France
[59] Laboratory for Particle Physics and Cosmology, Harvard University, Cambridge MA, United States
[60] [(a)] Kirchhoff-Institut für Physik, Ruprecht-Karls-Universität Heidelberg, Heidelberg; [(b)] Physikalisches Institut, Ruprecht-Karls-Universität Heidelberg, Heidelberg; [(c)] ZITI Institut für technische Informatik, Ruprecht-Karls-Universität Heidelberg, Mannheim, Germany
[61] Faculty of Applied Information Science, Hiroshima Institute of Technology, Hiroshima, Japan
[62] [(a)] Department of Physics, The Chinese University of Hong Kong, Shatin, N.T., Hong Kong, China; [(b)] Department of Physics, The University of Hong Kong, Hong Kong, China; [(c)] Department of Physics and Institute for Advanced Study, The Hong Kong University of Science and Technology, Clear Water Bay, Kowloon, Hong Kong, China
[63] Department of Physics, National Tsing Hua University, Taiwan, Taiwan
[64] Department of Physics, Indiana University, Bloomington IN, United States
[65] Institut für Astro- und Teilchenphysik, Leopold-Franzens-Universität, Innsbruck, Austria
[66] University of Iowa, Iowa City IA, United States
[67] Department of Physics and Astronomy, Iowa State University, Ames IA, United States
[68] Joint Institute for Nuclear Research, JINR Dubna, Dubna, Russia
[69] KEK, High Energy Accelerator Research Organization, Tsukuba, Japan
[70] Graduate School of Science, Kobe University, Kobe, Japan
[71] Faculty of Science, Kyoto University, Kyoto, Japan
[72] Kyoto University of Education, Kyoto, Japan
[73] Research Center for Advanced Particle Physics and Department of Physics, Kyushu University, Fukuoka, Japan
[74] Instituto de Física La Plata, Universidad Nacional de La Plata and CONICET, La Plata, Argentina
[75] Physics Department, Lancaster University, Lancaster, United Kingdom
[76] [(a)] INFN Sezione di Lecce; [(b)] Dipartimento di Matematica e Fisica, Università del Salento, Lecce, Italy
[77] Oliver Lodge Laboratory, University of Liverpool, Liverpool, United Kingdom
[78] Department of Experimental Particle Physics, Jožef Stefan Institute and Department of Physics, University of Ljubljana, Ljubljana, Slovenia
[79] School of Physics and Astronomy, Queen Mary University of London, London, United Kingdom
[80] Department of Physics, Royal Holloway University of London, Surrey, United Kingdom
[81] Department of Physics and Astronomy, University College London, London, United Kingdom
[82] Louisiana Tech University, Ruston LA, United States
[83] Laboratoire de Physique Nucléaire et de Hautes Energies, UPMC and Université Paris-Diderot and CNRS/IN2P3, Paris, France
[84] Fysiska institutionen, Lunds universitet, Lund, Sweden
[85] Departamento de Fisica Teorica C-15, Universidad Autonoma de Madrid, Madrid, Spain
[86] Institut für Physik, Universität Mainz, Mainz, Germany
[87] School of Physics and Astronomy, University of Manchester, Manchester, United Kingdom
[88] CPPM, Aix-Marseille Université and CNRS/IN2P3, Marseille, France
[89] Department of Physics, University of Massachusetts, Amherst MA, United States
[90] Department of Physics, McGill University, Montreal QC, Canada
[91] School of Physics, University of Melbourne, Victoria, Australia
[92] Department of Physics, The University of Michigan, Ann Arbor MI, United States
[93] Department of Physics and Astronomy, Michigan State University, East Lansing MI, United States
[94] [(a)] INFN Sezione di Milano; [(b)] Dipartimento di Fisica, Università di Milano, Milano, Italy
[95] B.I. Stepanov Institute of Physics, National Academy of Sciences of Belarus, Minsk, Belarus
[96] Research Institute for Nuclear Problems of Byelorussian State University, Minsk, Belarus
[97] Group of Particle Physics, University of Montreal, Montreal QC, Canada

[98] P.N. Lebedev Physical Institute of the Russian Academy of Sciences, Moscow, Russia
[99] Institute for Theoretical and Experimental Physics (ITEP), Moscow, Russia
[100] National Research Nuclear University MEPhI, Moscow, Russia
[101] D.V. Skobeltsyn Institute of Nuclear Physics, M.V. Lomonosov Moscow State University, Moscow, Russia
[102] Fakultät für Physik, Ludwig-Maximilians-Universität München, München, Germany
[103] Max-Planck-Institut für Physik (Werner-Heisenberg-Institut), München, Germany
[104] Nagasaki Institute of Applied Science, Nagasaki, Japan
[105] Graduate School of Science and Kobayashi-Maskawa Institute, Nagoya University, Nagoya, Japan
[106] [(a)] INFN Sezione di Napoli; [(b)] Dipartimento di Fisica, Università di Napoli, Napoli, Italy
[107] Department of Physics and Astronomy, University of New Mexico, Albuquerque NM, United States
[108] Institute for Mathematics, Astrophysics and Particle Physics, Radboud University Nijmegen/Nikhef, Nijmegen, Netherlands
[109] Nikhef National Institute for Subatomic Physics and University of Amsterdam, Amsterdam, Netherlands
[110] Department of Physics, Northern Illinois University, DeKalb IL, United States
[111] Budker Institute of Nuclear Physics, SB RAS, Novosibirsk, Russia
[112] Department of Physics, New York University, New York NY, United States
[113] Ohio State University, Columbus OH, United States
[114] Faculty of Science, Okayama University, Okayama, Japan
[115] Homer L. Dodge Department of Physics and Astronomy, University of Oklahoma, Norman OK, United States
[116] Department of Physics, Oklahoma State University, Stillwater OK, United States
[117] Palacký University, RCPTM, Olomouc, Czech Republic
[118] Center for High Energy Physics, University of Oregon, Eugene OR, United States
[119] LAL, Univ. Paris-Sud, CNRS/IN2P3, Université Paris-Saclay, Orsay, France
[120] Graduate School of Science, Osaka University, Osaka, Japan
[121] Department of Physics, University of Oslo, Oslo, Norway
[122] Department of Physics, Oxford University, Oxford, United Kingdom
[123] [(a)] INFN Sezione di Pavia; [(b)] Dipartimento di Fisica, Università di Pavia, Pavia, Italy
[124] Department of Physics, University of Pennsylvania, Philadelphia PA, United States
[125] National Research Centre "Kurchatov Institute" B.P.Konstantinov Petersburg Nuclear Physics Institute, St. Petersburg, Russia
[126] [(a)] INFN Sezione di Pisa; [(b)] Dipartimento di Fisica E. Fermi, Università di Pisa, Pisa, Italy
[127] Department of Physics and Astronomy, University of Pittsburgh, Pittsburgh PA, United States
[128] [(a)] Laboratório de Instrumentação e Física Experimental de Partículas - LIP, Lisboa; [(b)] Faculdade de Ciências, Universidade de Lisboa, Lisboa; [(c)] Department of Physics, University of Coimbra, Coimbra; [(d)] Centro de Física Nuclear da Universidade de Lisboa, Lisboa; [(e)] Departamento de Fisica, Universidade do Minho, Braga; [(f)] Departamento de Fisica Teorica y del Cosmos and CAFPE, Universidad de Granada, Granada; [(g)] Dep Fisica and CEFITEC of Faculdade de Ciencias e Tecnologia, Universidade Nova de Lisboa, Caparica, Portugal
[129] Institute of Physics, Academy of Sciences of the Czech Republic, Praha, Czech Republic
[130] Czech Technical University in Prague, Praha, Czech Republic
[131] Charles University, Faculty of Mathematics and Physics, Prague, Czech Republic
[132] State Research Center Institute for High Energy Physics (Protvino), NRC KI, Russia
[133] Particle Physics Department, Rutherford Appleton Laboratory, Didcot, United Kingdom
[134] [(a)] INFN Sezione di Roma; [(b)] Dipartimento di Fisica, Sapienza Università di Roma, Roma, Italy
[135] [(a)] INFN Sezione di Roma Tor Vergata; [(b)] Dipartimento di Fisica, Università di Roma Tor Vergata, Roma, Italy
[136] [(a)] INFN Sezione di Roma Tre; [(b)] Dipartimento di Matematica e Fisica, Università Roma Tre, Roma, Italy
[137] [(a)] Faculté des Sciences Ain Chock, Réseau Universitaire de Physique des Hautes Energies - Université Hassan II, Casablanca; [(b)] Centre National de l'Energie des Sciences Techniques Nucleaires, Rabat; [(c)] Faculté des Sciences Semlalia, Université Cadi Ayyad, LPHEA-Marrakech; [(d)] Faculté des Sciences, Université Mohamed Premier and LPTPM, Oujda; [(e)] Faculté des sciences, Université Mohammed V, Rabat, Morocco
[138] DSM/IRFU (Institut de Recherches sur les Lois Fondamentales de l'Univers), CEA Saclay (Commissariat à l'Energie Atomique et aux Energies Alternatives), Gif-sur-Yvette, France
[139] Santa Cruz Institute for Particle Physics, University of California Santa Cruz, Santa Cruz CA, United States
[140] Department of Physics, University of Washington, Seattle WA, United States
[141] Department of Physics and Astronomy, University of Sheffield, Sheffield, United Kingdom
[142] Department of Physics, Shinshu University, Nagano, Japan
[143] Department Physik, Universität Siegen, Siegen, Germany
[144] Department of Physics, Simon Fraser University, Burnaby BC, Canada
[145] SLAC National Accelerator Laboratory, Stanford CA, United States
[146] [(a)] Faculty of Mathematics, Physics & Informatics, Comenius University, Bratislava; [(b)] Department of Subnuclear Physics, Institute of Experimental Physics of the Slovak Academy of Sciences, Kosice, Slovak Republic
[147] [(a)] Department of Physics, University of Cape Town, Cape Town; [(b)] Department of Physics, University of Johannesburg, Johannesburg; [(c)] School of Physics, University of the Witwatersrand, Johannesburg, South Africa
[148] [(a)] Department of Physics, Stockholm University; [(b)] The Oskar Klein Centre, Stockholm, Sweden
[149] Physics Department, Royal Institute of Technology, Stockholm, Sweden
[150] Departments of Physics & Astronomy and Chemistry, Stony Brook University, Stony Brook NY, United States
[151] Department of Physics and Astronomy, University of Sussex, Brighton, United Kingdom
[152] School of Physics, University of Sydney, Sydney, Australia
[153] Institute of Physics, Academia Sinica, Taipei, Taiwan
[154] Department of Physics, Technion: Israel Institute of Technology, Haifa, Israel
[155] Raymond and Beverly Sackler School of Physics and Astronomy, Tel Aviv University, Tel Aviv, Israel
[156] Department of Physics, Aristotle University of Thessaloniki, Thessaloniki, Greece
[157] International Center for Elementary Particle Physics and Department of Physics, The University of Tokyo, Tokyo, Japan
[158] Graduate School of Science and Technology, Tokyo Metropolitan University, Tokyo, Japan
[159] Department of Physics, Tokyo Institute of Technology, Tokyo, Japan
[160] Tomsk State University, Tomsk, Russia
[161] Department of Physics, University of Toronto, Toronto ON, Canada
[162] [(a)] INFN-TIFPA; [(b)] University of Trento, Trento, Italy
[163] [(a)] TRIUMF, Vancouver BC; [(b)] Department of Physics and Astronomy, York University, Toronto ON, Canada
[164] Faculty of Pure and Applied Sciences, and Center for Integrated Research in Fundamental Science and Engineering, University of Tsukuba, Tsukuba, Japan
[165] Department of Physics and Astronomy, Tufts University, Medford MA, United States
[166] Department of Physics and Astronomy, University of California Irvine, Irvine CA, United States
[167] [(a)] INFN Gruppo Collegato di Udine, Sezione di Trieste, Udine; [(b)] ICTP, Trieste; [(c)] Dipartimento di Chimica, Fisica e Ambiente, Università di Udine, Udine, Italy
[168] Department of Physics and Astronomy, University of Uppsala, Uppsala, Sweden
[169] Department of Physics, University of Illinois, Urbana IL, United States
[170] Instituto de Fisica Corpuscular (IFIC), Centro Mixto Universidad de Valencia - CSIC, Spain

[171] Department of Physics, University of British Columbia, Vancouver BC, Canada
[172] Department of Physics and Astronomy, University of Victoria, Victoria BC, Canada
[173] Department of Physics, University of Warwick, Coventry, United Kingdom
[174] Waseda University, Tokyo, Japan
[175] Department of Particle Physics, The Weizmann Institute of Science, Rehovot, Israel
[176] Department of Physics, University of Wisconsin, Madison WI, United States
[177] Fakultät für Physik und Astronomie, Julius-Maximilians-Universität, Würzburg, Germany
[178] Fakultät für Mathematik und Naturwissenschaften, Fachgruppe Physik, Bergische Universität Wuppertal, Wuppertal, Germany
[179] Department of Physics, Yale University, New Haven CT, United States
[180] Yerevan Physics Institute, Yerevan, Armenia
[181] Centre de Calcul de l'Institut National de Physique Nucléaire et de Physique des Particules (IN2P3), Villeurbanne, France

[a] Also at Department of Physics, King's College London, London, United Kingdom.
[b] Also at Institute of Physics, Azerbaijan Academy of Sciences, Baku, Azerbaijan.
[c] Also at Novosibirsk State University, Novosibirsk, Russia.
[d] Also at TRIUMF, Vancouver BC, Canada.
[e] Also at Department of Physics & Astronomy, University of Louisville, Louisville, KY, United States of America.
[f] Also at Physics Department, An-Najah National University, Nablus, Palestine.
[g] Also at Department of Physics, California State University, Fresno CA, United States of America.
[h] Also at Department of Physics, University of Fribourg, Fribourg, Switzerland.
[i] Also at II Physikalisches Institut, Georg-August-Universität, Göttingen, Germany.
[j] Also at Departament de Fisica de la Universitat Autonoma de Barcelona, Barcelona, Spain.
[k] Also at Departamento de Fisica e Astronomia, Faculdade de Ciencias, Universidade do Porto, Portugal.
[l] Also at Tomsk State University, Tomsk, Russia.
[m] Also at The Collaborative Innovation Center of Quantum Matter (CICQM), Beijing, China.
[n] Also at Universita di Napoli Parthenope, Napoli, Italy.
[o] Also at Institute of Particle Physics (IPP), Canada.
[p] Also at Horia Hulubei National Institute of Physics and Nuclear Engineering, Bucharest, Romania.
[q] Also at Department of Physics, St. Petersburg State Polytechnical University, St. Petersburg, Russia.
[r] Also at Borough of Manhattan Community College, City University of New York, New York City, United States of America.
[s] Also at Department of Physics, The University of Michigan, Ann Arbor MI, United States of America.
[t] Also at Department of Financial and Management Engineering, University of the Aegean, Chios, Greece.
[u] Also at Centre for High Performance Computing, CSIR Campus, Rosebank, Cape Town, South Africa.
[v] Also at Louisiana Tech University, Ruston LA, United States of America.
[w] Also at Institucio Catalana de Recerca i Estudis Avancats, ICREA, Barcelona, Spain.
[x] Also at Graduate School of Science, Osaka University, Osaka, Japan.
[y] Also at Fakultät für Mathematik und Physik, Albert-Ludwigs-Universität, Freiburg, Germany.
[z] Also at Institute for Mathematics, Astrophysics and Particle Physics, Radboud University Nijmegen/Nikhef, Nijmegen, Netherlands.
[aa] Also at Department of Physics, The University of Texas at Austin, Austin TX, United States of America.
[ab] Also at Institute of Theoretical Physics, Ilia State University, Tbilisi, Georgia.
[ac] Also at CERN, Geneva, Switzerland.
[ad] Also at Georgian Technical University (GTU),Tbilisi, Georgia.
[ae] Also at Ochadai Academic Production, Ochanomizu University, Tokyo, Japan.
[af] Also at Manhattan College, New York NY, United States of America.
[ag] Also at Academia Sinica Grid Computing, Institute of Physics, Academia Sinica, Taipei, Taiwan.
[ah] Also at The City College of New York, New York NY, United States of America.
[ai] Also at School of Physics, Shandong University, Shandong, China.
[aj] Also at Departamento de Fisica Teorica y del Cosmos and CAFPE, Universidad de Granada, Granada, Portugal.
[ak] Also at Department of Physics, California State University, Sacramento CA, United States of America.
[al] Also at Moscow Institute of Physics and Technology State University, Dolgoprudny, Russia.
[am] Also at Departement de Physique Nucleaire et Corpusculaire, Université de Genève, Geneva, Switzerland.
[an] Also at International School for Advanced Studies (SISSA), Trieste, Italy.
[ao] Also at Institut de Física d'Altes Energies (IFAE), The Barcelona Institute of Science and Technology, Barcelona, Spain.
[ap] Also at School of Physics, Sun Yat-sen University, Guangzhou, China.
[aq] Also at Institute for Nuclear Research and Nuclear Energy (INRNE) of the Bulgarian Academy of Sciences, Sofia, Bulgaria.
[ar] Also at Faculty of Physics, M.V.Lomonosov Moscow State University, Moscow, Russia.
[as] Also at Institute of Physics, Academia Sinica, Taipei, Taiwan.
[at] Also at National Research Nuclear University MEPhI, Moscow, Russia.
[au] Also at Department of Physics, Stanford University, Stanford CA, United States of America.
[av] Also at Institute for Particle and Nuclear Physics, Wigner Research Centre for Physics, Budapest, Hungary.
[aw] Also at Giresun University, Faculty of Engineering, Turkey.
[ax] Also at CPPM, Aix-Marseille Université and CNRS/IN2P3, Marseille, France.
[ay] Also at Department of Physics, Nanjing University, Jiangsu, China.
[az] Also at University of Malaya, Department of Physics, Kuala Lumpur, Malaysia.
[ba] Also at LAL, Univ. Paris-Sud, CNRS/IN2P3, Université Paris-Saclay, Orsay, France.
[bb] Also at PKU-CHEP.
[*] Deceased.